NUMERICAL SIMULATION TO STUDY THE EFFECT OF BIASING AND TEMPERATURE ON CARBON DEPOSITION DURING GRAPHENE GROWTH USING $Ar/C_2H_2/H_2$ IN PECVD

A DISSERTATION

SUBMITTED IN PARTIAL FULFILLMENT OF THE REQUIREMENTS
FOR THE AWARD OF DEGREE
OF

MASTER OF TECHNOLOGY

IN

NANOSCIENCE AND TECHNOLOGY

Submitted By

MANISH KUMAR

(Roll No. 2K16/NST/04)

Under the supervision of

PROF. (DR.) SURESH C. SHARMA

DEPARTMENT OF APPLIED PHYSICS

Delhi Technological University

(Formerly Delhi College of Engineering)

Bawana Road, Delhi-110042

JUNE,2018

DELHI TECHNOLOGICAL UNIVERSITY

(Formerly Delhi College of Engineering)

Bawana Road, Delhi-110042

CANDIDATE'S DECLARATION

I, Manish Kumar, Roll No. 2K16/NST/04 of M.Tech. Nanoscience and Technology, hereby declare that the project Dissertation titled **"Numerical simulation to study the effect of biasing and temperature on carbon deposition during graphene growth using Ar/C_2H_2/H_2 in PECVD"** which is submitted by me to the Department of Applied Physics, Delhi Technological University, Delhi in partial fulfillment of the requirement for the award of the degree of Master of technology, is original and not copied from any source without proper citation. This work has not been used for the award of any Degree, Diploma Associateship, Fellowship or other similar title or recognition.

Place, Delhi, INDIA **Manish Kumar**

Date:

DELHI TECHNOLOGICAL UNIVERSITY

(Formerly Delhi College of Engineering)

Bawana Road, Delhi-110042

CERTIFICATE

I hereby certify that the Project Dissertation titled **"Numerical simulation to study the effect of biasing and temperature on carbon deposition during graphene growth using Ar/C_2H_2/H_2 in PECVD"** by **Manish Kumar**, Roll No. **2K16/NST/04**, Department of Applied Physics, Delhi in partial fulfillment of the requirement for the award of the degree of Master of Technology, is a record of the project work carried out by the student under my supervision. To the best of my knowledge, this work has not been submitted in parts or full for any Degree or Diploma to this University or elsewhere.

Place, Delhi, India
Date:

Prof. (Dr.) Suresh C. Sharma
HOD, Applied Physics
Delhi Technological University
Delhi, INDIA

ACKNOWLEDGEMENT

First, I would like to thank **my family**. Without their love and support over the years, none of this would have been possible. They have always been there for me and I am thankful for everything they have helped me achieve.

I wish to express my deep sense of gratitude and veneration to my supervisor, **Prof. (Dr.) Suresh C. Sharma**, Head of Department, Department of Applied Physics, Delhi Technological University, Delhi, for his perpetual encouragement, constant guidance, valuable suggestions and continued motivation, which has enabled me to complete this work.

I am also thankful to all the faculty members for their constant guidance and facilities to carry out my work. I would like to convey special thanks to **Mr. Ravi Gupta and Ms. Neha Gupta** and all fellow members of Ph.D. for their constant support and guidance.

Finally, I would like to thank my dear friends **Sagar Khanna, Astha Srivastava, Saumya Tripathi and Anurag.** For coming to lab daily, and staying up till I leave, we shared the same story and worked hard together. This experience would not have been fun without them.

Manish Kumar
M.Tech (NST), DTU
Roll NO. 2K16/NST/04

Abstract

NUMERICAL SIMULATION TO STUDY THE EFFECT OF BIASING AND TEMPERATURE ON CARBON DEPOSITION DURING GRAPHENE GROWTH USING $Ar/C_2H_2/H_2$ IN PECVD

MANISH KUMAR
DEPARTMENT OF APPLIED PHYSICS
DELHI TECHNOLOGICAL UNIVERSITY
SUPERVISOR: PROF. (DR.) SURESH C. SHARMA

Graphene is excellent material in sense of their wide range of applications in electronic devices as ultrafast transistors, electron field emitters, microelectrochemical systems, biochemical operations, optoelectronics, composite materials, photovoltaic cells, and energy storage etc. such extraordinary applications are due to unique geometry, high mechanical strength, high thermal and electrical properties, high chemical stability and impermeability. There are various synthesis techniques for the synthesis of graphene. The most commonly used and effective technique is chemical vapor deposition. Among various CVD techniques, Thermal Chemical Vapor Deposition and Plasma Enhanced Chemical Vapor Deposition are currently using throughout. Among these two CVD techniques, Thermal CVD systems are used at industrial level for large-scale synthesis of CNTs and Graphene. But there is one drawback with Thermal CVD is that the temperature in the chamber, especially near the substrate increase up to a very high value that the substrate decomposes thermally and left unusable for further use. In this case, Plasma Enhanced CVD techniques come into use as the temperature in the PECVD chamber does not exceed above 600^oc. PECVD technique can be worked in low temperature while the deposition rate is equivalent to other CVD forms.

In this study, we have simulated the Plasma enhanced CVD to grow a horizontal planar layer of graphene on the substrate and vertically aligned graphene at the edges of the substrate. The graphene sheets were deposited on 200nm thick nickel catalyst sheet on a silicon substrate from 300K to 723K using acetylene (C_2H_2) as the carbon source in an argon

(Ar) and hydrogen (H_2) atmosphere. Ionization of Argon gas takes place by transformer action leading to the generation of plasma. Under the effect of the plasma, the carbon-containing gas goes through both ion-induced and thermal decomposition. The plasma also causes the nickel catalyst film to turn into nanoparticles, which acts as the active sites for carbon cluster or island formation. As the carbon fluxes reach the catalyst they diffuse into the catalyst nanoparticles and when they cool down, cluster or island formation occurs. The dispersion of these islands or cluster leads to the formation of the graphene layer.

As the biasing of substrate increases from zero bias to -50 V DC the effective etching of catalyst surface increases, leading to decrease in thickness of planar graphene as well as a reduction in height of vertical graphene at the edges. Increase in temperature allows more carbon fluxes to diffuse into the catalyst nanoparticles, leading to increase in the thickness of planar graphene as well as vertically aligned graphenes at the edges.

CONTENTS

Candidate's Declaration I

Certificate II

Acknowledgement III

Abstract IV

Contents VI

List of Figures VIII

List of Symbols, abbreviations XI

CHAPTER 1 INTRODUCTION 1

1.1 Background 1

12 Carbon nanostructures 2

1.3 Graphene 3

1.4 Properties of Graphene 5

1.4.1 General Properties 6

1.4.2 Strength and Stiffness 6

1.4.3 Thermal Conductivity 6

1.4.4 Impermeability 6

1.4.5 Holding Capacity 7

1.5 Synthesis of Graphene 7

1.6 Chemical Vapor Deposition 7

1.7 Thermal Chemical Vapor Deposition 8

1.8 Plasma Enhanced Chemical Vapor Deposition 9

1.9 Applications 10

1.9.1 Biological Engineering 11

1.9.2 Optical Electronics 12

1.9.4 Photovoltaic Cells 13
1.9.4 Energy Storage 13
1.10 COMSOL Multiphysics 14

CHAPTER 2 SIMULATIONAL MODEL 15
2.1 Model Assumptions 16
2.2 Geometry and Materials 17
2.3 Physics and Equation Involved 25
2.4 Reactions Considered 27

CHAPTER 3 RESULTS AND DISCUSSIONS 31
3.1 Plasma Chemistry and Surface Phenomenon 31
3.2 Accumulated Carbon Growth on Substrate 37
3.2.1 Varying Substrate Bias 37
3.2.2 Varying Temperature 42

CHAPTER 4 CONCLUSION 47
4.1 Summary 47
4.2 Future Outlook 48

CHAPTER 5 REFERENCES 49

List of figures

Figure 1.1 Structure of Carbon Nano-tubes 3

Figure 1.2 Structure of Fullerene 3

Figure 1.3 Structural arrangement of carbon atoms in a) Diamond and b) Graphite 4

Figure 1.4 Structure of Graphene 5

Figure 1.5 Process flow in Chemical Vapor Deposition 8

Figure 1.6 Schematic Diagram of Thermal Chemical Vapor Deposition 9

Figure 1.7 Schematic Diagram of Plasma Enhanced Chemical Vapor Deposition 10

Figure 1.8 Various Applications of Graphene 11

Figure 2.1 Schematic Diagram of 2D axis-symmetric PECVD model considered for simulation 18

Figure 2.2 Schematic Diagram of actual 3D PECVD model 19

Figure 2.3 Meshing of 2D axis-symmetric PECVD Model 20

Figure 2.3.1 Meshing near Power coil and dielectric region 20

Figure 2.3.2 Meshing near the substrate and biasing coil 21

Figure 2.4 Schematic representation of the formation of graphene sheet under plasma 21

Figure 2.5 Flow chart for the mechanism of growth of carbon nanostructures by PECVD technique 22

Figure 2.6 Schematic showing the mechanism for CVD graphene growth 23

Figure 3.1.1 C_2H Number Density at 300K 32

Figure 3.1.2 C_2H Number Density at 723K 32

Figure 3.2.1 C_2H_2 Ion Density at 300K 33

Figure 3.2.2 C_2H_2 Ion Density at 723K 33

Figure 3.3.2 C_2H_3 Ion Density at 300K 34

Figure 3.3.2 C_2H_3 Ion Density at 723K 35

Figure 3.4.1 Number Densities of Various Ions at 300 k and 723 K 36

Figure 3.4.2 Number Densities of various neutral species at 300 K and 723 K 36

Figure 3.5.1 Accumulated carbon growth height -50 V DC bias at 723K 37

Figure 3.5.2 Accumulated carbon growth height without bias and 723K 38

Figure 3.6.1 Accumulated carbon growth 3D at -50V DC bias at 723K 38

Figure 3.6.2 Accumulated carbon growth 3D without bias at 723K 39

Figure3.7.1 Accumulated carbon growth rate at -50V DC bias at 723K 40

Figure 3.7.2 Accumulated carbon growth rate without bias at 723K 41

Figure 3.8.1 Accumulated Carbon Growth at 300 K and -50V DC 42

Figure 3.8.2 Accumulated Carbon Growth at 723 K and -50V DC 43

Figure 3.9.1 Accumulated Carbon Growth 3D at 300 K and -50 V DC 43

Figure 3.9.2 Accumulated Carbon Growth 3D at 723 K and -50 V DC 44

Figure 3.10.1 Accumulated Carbon Growth Rate at 300 K and -50V DC 45

Figure 3.10.2 Accumulated Carbon Growth Rate at 723 K and -50V DC 46

Abbreviation

CNT= Carbon Nano Tube

T-CVD=Thermal Chemical vapor deposition

PECVD= Plasma Enhanced Chemical Vapor Deposition

RF= Radiofrequency

ICP= Inductively Coupled Plasma

PVD= Physical Vapor Deposition

ITO= Indium Tin Oxide

Ar= Argon

HST= Heavy Species Transport

DC= Direct Current

2D= Two Dimensional

3D= Three Dimensional

C_2H_2 Acetylene

(S)= Adsorbed Species

(b)= Bulk Species

1

INTRODUCTION

1.1 BACKGROUND

Carbon nanostructures such as graphene, carbon Nano-films, and carbon nanotubes have recently been extensively explored for the fabrication of various Nano-electronic devices such as electron field emitters[1], ultrafast transistors[2] and micro-electrochemical systems[3], excellent electron field enhancing properties of the carbon nanostructures are credited to their exclusive structural and size-dependent electronic properties[4], vertically aligned carbon nanostructures are also mechanically and chemically tough and are able to produce huge currents at low electric fields[5]. Graphenes are found to show excellent properties which make them useful in catalysis, gas separation, analysis, energy storage etc[6-10]. It has been observed that Nano-films of certain materials other than carbon like cadmium telluride and zinc selenide have application in detection of harmful gases like carbon monoxide [11,12].

The two major techniques, namely thermal chemical vapor deposition and plasma-enhanced chemical vapor deposition [T-CVD and PECVD respectively] have recently gained

popularity as the most preferred and widely used synthesis techniques [13-15]. PECVD is preferred over T-CVD as PECVD offers the vertically oriented growth of carbon nanostructures due to the alignment force exerted by the electric field induced in the plasma sheath region and gaseous source are activated due to electron impact reaction in the plasma at a low temperature and low pressure. In PECVD, the gaseous sources exist in the ionized state in the plasma. The common source of plasma is Microwave-PECVD, Radio Frequency-PECVD, Direct Current-PECVD and Inductively Coupled-PECVD (ICP). Stability of the plasma is primary requirement to maintain the ignition of the plasma which leads to much-enhanced growth. Thus, plasma is operated at low pressure because at high pressure, the collision between electrons and species is inelastic which leads to the loss of electron energy and stability of plasma. In reactive plasma, highly reactive positively charged ions and neutral species are generated due to collisions between electron and other gaseous species without much rise in gas temperature. The composition of the plasma depends upon the reaction between electrons and gaseous species. The electric field in the plasma directly influences the electron density and temperature which ultimately affects the dissociation and ionization of neutral gaseous species. Many parameters such as; temperature, biasing, power, power, pressure and flow rate etc. critically influence the plasma properties.

Graphene (carbon Nano-films) possesses a number of incredible properties, previously not witnessed at the Nanoscale. The observations include quantum Hall Effect at room-temperature, high electron mobility along with ballistic transport, large mean free paths for the electron, higher thermal conductivity, mechanical strength, and tremendous flexibility are among the striking properties of graphene[16-18].

1.2 CARBON NANO-STRUCTURES

Carbon is found in two basic types but having different forms and structure (or allotropes). 1) Graphite (the soft, black stuff in pencil "leads") and 2) diamond (the super-hard and sparkly crystals). The most amazing thing about both these allotropes are both being different materials are made up of same carbon atoms. The atoms inside graphite and diamond are arranged in different ways. And this different arrangement gives the two allotropes their distinctive and completely different properties.

In the last few decades, various other allotropes with amazingly different properties have been discovered. Fullerene is hollow cages of carbon atoms which were discovered in the year 1985. Followed by the Buckyball, arranged in a kind of 3D football-shaped of 60 carbon atoms). The carbon nanotubes were discovered in 1991; are thin sheets of carbon atoms twisted and curled into amazingly thin tubes of diameter in nanometer and finally, graphene (discovered in 2004) being the most recently discovered carbon structure.

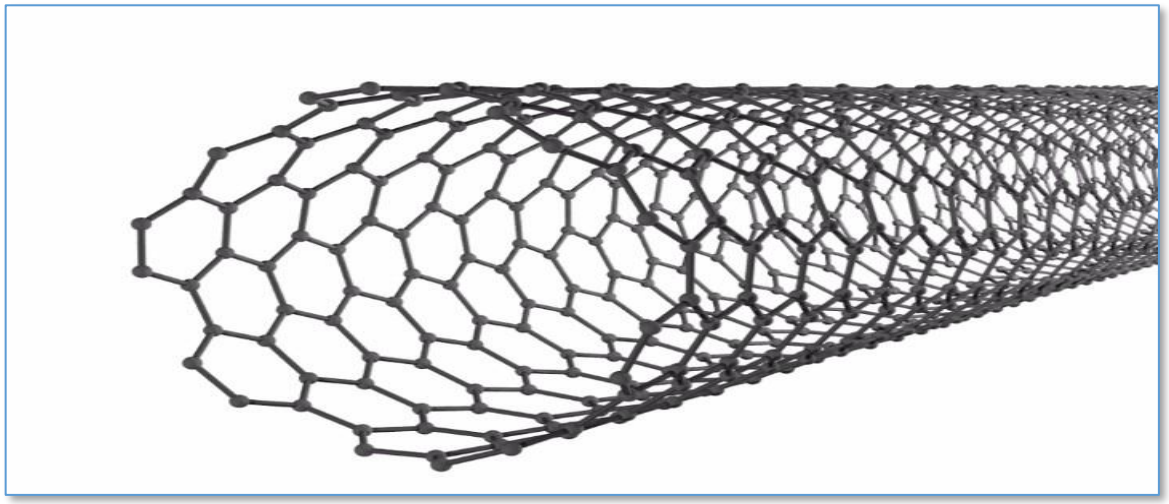

Figure 1.1 Structure of Carbon Nano-tubes by www.scienceabc.com

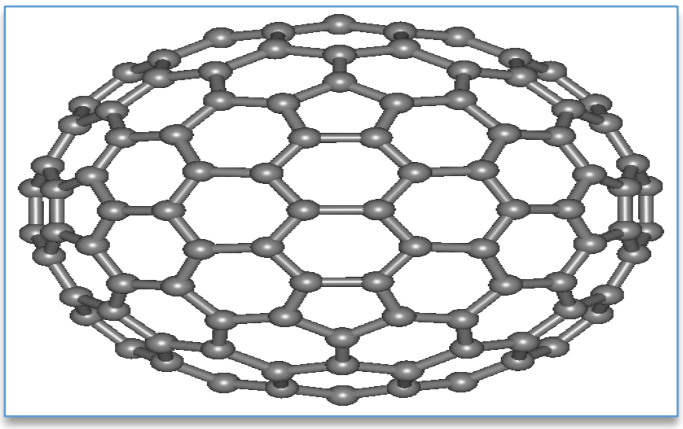

Figure 1.2 Structure of Fullerene by www.scienceabc.com

The crystal lattice structure of these materials makes them different. Diamond and graphite are the three-dimensional structure of carbon atoms arranged as shown in Figure

1.3. In diamond, the carbon atoms are strongly bonded in three-dimensional tetrahedrons structure, whereas in graphite, the carbon atoms are bonded tightly in two-dimensional layers, these layers are held above and below by relatively weak forces.

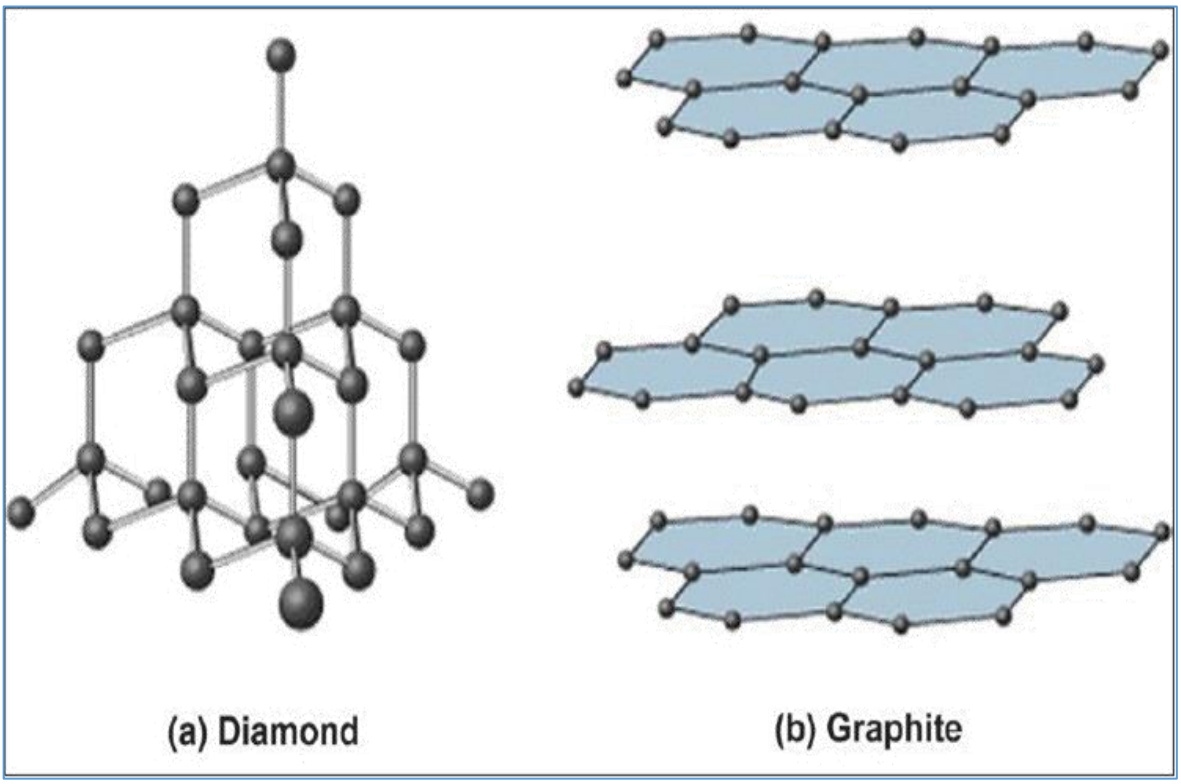

Figure 1.3 Structural arrangement of carbon atoms in a) Diamond and b) Graphite from www.brainly.in

1.3 GRAPHENE

Graphene is a single layer of graphite having a crystalline structure. It is two-dimensional. In other words, the carbon atoms in graphene are placed out flat horizontally or vertically. Each layer of graphene is made of hexagonal "rings" of carbon atoms just like graphite. These carbon atoms look like lots of benzene rings connected together. The only difference being hydrogen atoms replaced by carbon, giving graphene a honeycomb-like appearance

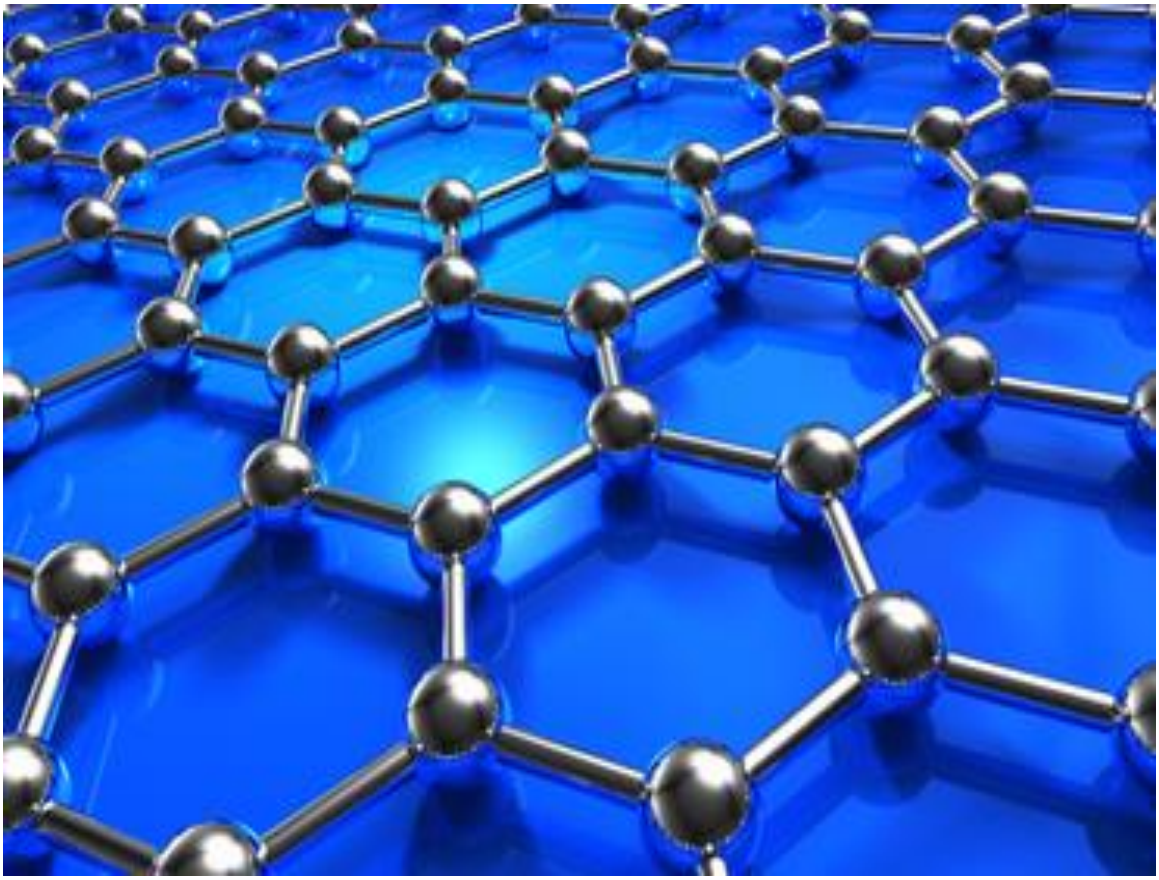

Figure 1.4 Structure of Graphene from www.scienceabc.com

1.4 PROPERTIES OF GRAPHENE

The most important properties of graphene are:

1.4.1 General properties

- Graphene is a remarkably pure substance because of its largely simple and ordered structure based on a compact, regular arrangements of the atom and atomic bonding,
- Carbon is a nonmetal but graphene is not. In fact, it is conductive. Graphene behaves much more like a metal (though it conducts electricity in a very different way), and this led to call it more as a semi-metal or a semiconductor (being a material in between a conductor and an insulator, such as germanium or silicon).

1.4.2 Strength and stiffness

- **Soft**: The arrangements of carbon layers inside a graphite is such that it shaves off quite easily. If one scribbles with a soft pencil (somewhat like a 4B), you'll notice that graphite is extremely soft.
- **Strong**: The carbon atoms within the graphitic layers are so tightly bonded. So, in the same way, carbon nanotubes, unlike normal graphite material, graphene is super-strong. Way stronger than diamond. Graphene is supposed to be by far the strongest material discovered yet. It is some 200 times stronger than the steel.
- **Stretchable**: It is both stiff and elastic like a rubber, so it can be stretched by an amazing 20-25 % of its length without breaking it. This is because of the horizontal planes of carbon atoms inside the graphene, that can flex easily without breaking apart the atoms

  The implementation of the super-strong properties of graphene is still unexplored and have not been used sufficiently so far, but one likelihood of it is mixing graphene with other materials to make composites that are tougher and harder, but at the same time also thinner and lighter than all materials known so far.

1.4.3 Thermal conductivity

Graphene is better at carrying heat or we can say that graphene has very high thermal conductivity compared to any other material. The thermal conductivity of graphene is even better by far than other good heat conductors such as silver and copper. By implementing graphene with other materials as a composite, the thermal conductivity can be much enhanced. By using graphene, we can provide thermal resistance to other materials that were vulnerable to heat.

1.4.4 Impermeability

- The sheets of graphene have a closely interweave carbon atoms which they can work like atomic nets which are super fine. Thus, stopping other materials from passing through it. That helps graphene being useful in trapping and detection of gases.

- **Holding capacity**: Graphene is amazingly capable of trapping and storing gases such as Hydrogen that leaks very easily when stored in a normal container. The drawbacks of storing hydrogen as a fuel safely were holding it to be used as fuel in electric cars.

1.5 SYNTHESIS OF GRAPHENE

Graphene mono-layers can be produced in different ways. But certainly, the most prevalent way to produce graphene now a day in time is with the help of a process called chemical vapor deposition. Chemical vapor deposition (CVD), It is a method that can mass produce comparatively high-quality graphene with potentially a large scale. The Chemical vapor deposition process is reasonably forthright; however, some specialized and costlier equipment is necessary in order to make high-quality graphene. It is more important to strictly follow the guidelines set parameters concerning the volume of gas, pressure, temperature, and the time duration of the operation.

1.6 CHEMICAL VAPOUR DEPOSITION

CVD is a process of deposition of gaseous reactants on the substrate. CVD works by coalescing the gas molecules provided through pumps in a CVD reaction chamber which are initially operated at ambient temperature. When the constituent gases interact with the substrate present in the plasma reaction chamber, a set of reactions occur that initiates thin film on the substrate surface. The waste gases are then pumped from the reaction chamber. The substrate temperature is the main condition that governs the type of reaction that will happen in CVD, so it plays a vital role. Thus, the temperature must be correct.

During the process of deposition in CVD, the substrate with a small amount of material very slowly at a rate described in microns of deposition per hour. The process is similar to physical vapor deposition (PVD). In this method, there is just one difference, that the precursors being solid compounds, rather than gases. Therefore, the process is somewhat different. These solid compounds get vaporized and then settles down toward substrate. Leading to deposition via condensation.

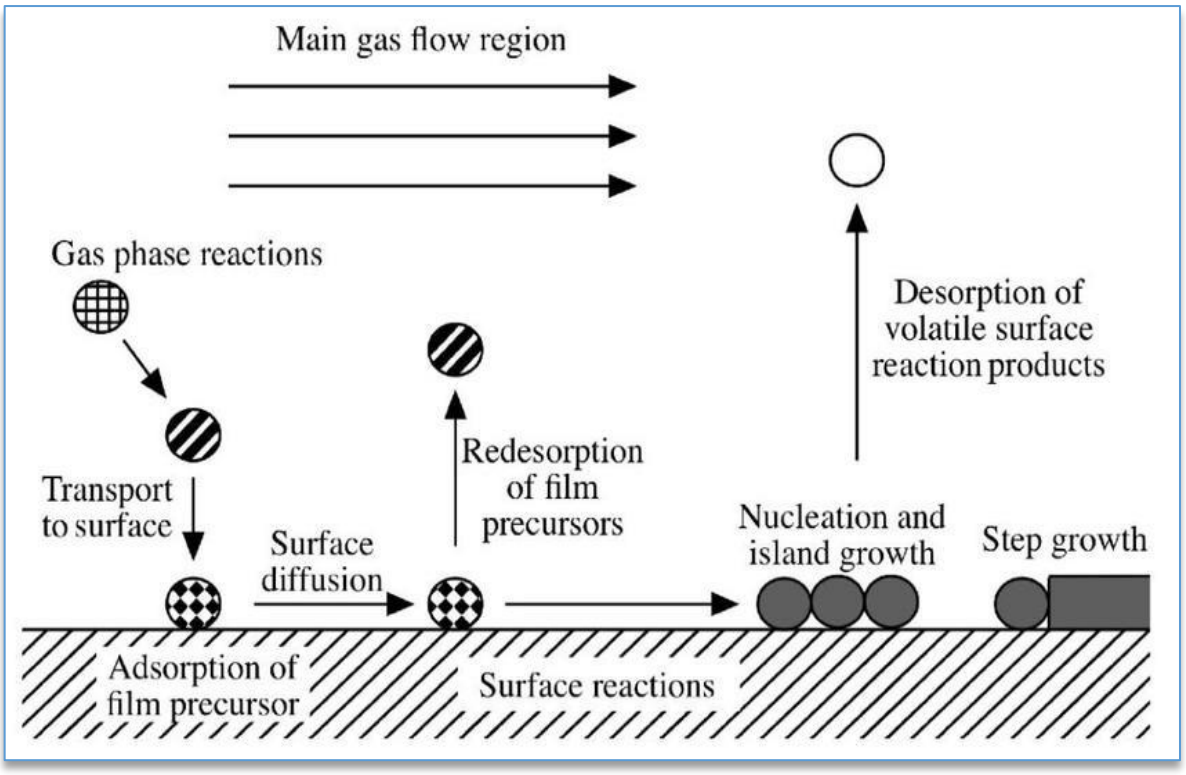

Figure 1.5 Process flow in Chemical Vapor Deposition

1.7 THERMAL CHEMICAL VAPOR DEPOSITION

In Thermal Chemical vapor deposition technique, the deposited film experiences thermal surface energy provided either by a substrate heating source or by condensing atoms, which initiates the thin film deposition. This thermal surface energy transfers enough mobility to atoms on the surface such that there is a uniform growth of film and good surface area. Higher the temperature during deposition, the better is the film deposition on the substrate. The substrate temperature aids to both atom surface mobility and the surface chemistry alone. Here the main thing of interest is the ratio of the substrate temperature to the melting point of the deposited film. It is important to keep a track of the temperature to protect the substrate from melting. The discerning nature of thermal chemical vapor deposition is to deposit thin films only on substrate surfaces above a fixed critical temperature. This phenomenon can be taken a step by incorporating catalytic surfaces that will decompose reactants at a relatively lower temperature than the non-catalytic surfaces.

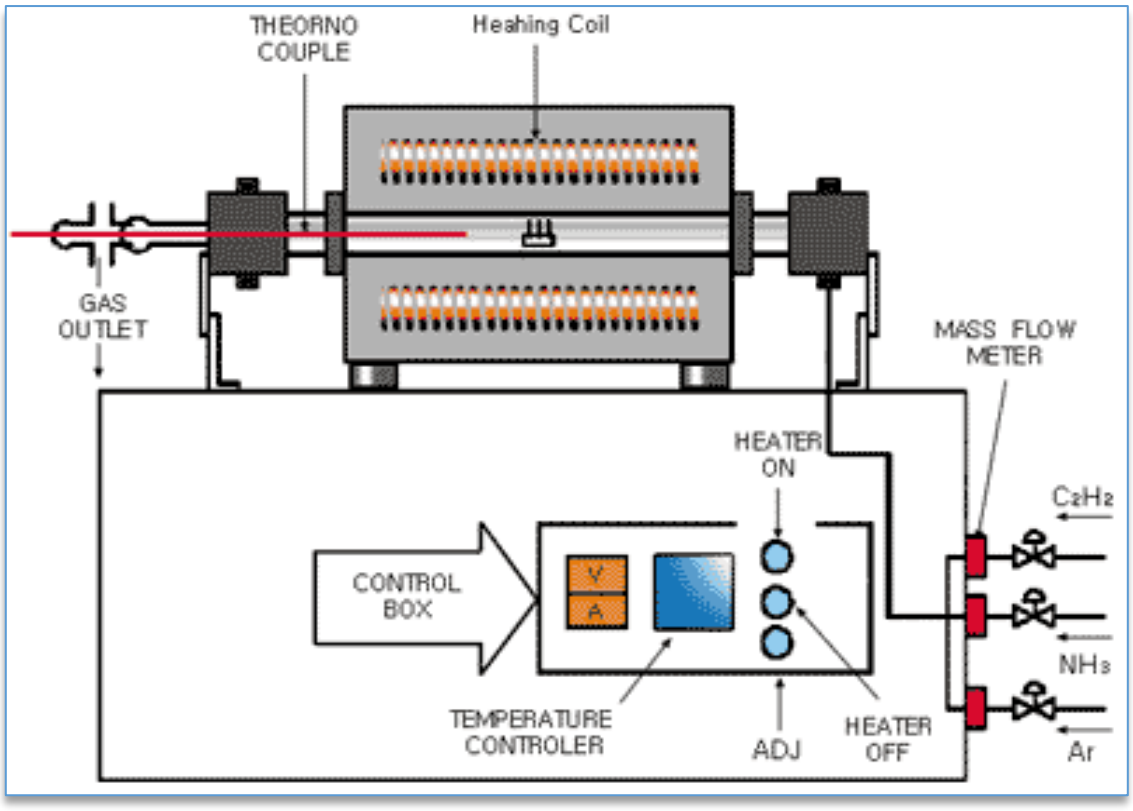

Figure 1.6 Schematic Diagram of Thermal Chemical Vapor Deposition by Nayan Das from www.researchgate.com

1.8 PLASMA ENHANCED CHEMICAL VAPOR DEPOSITION

Plasma enhanced chemical vapor deposition (PECVD) (also termed as plasma assisted, PACVD) is a technique where the activation energy required for the chemical vapor reaction to happen is attained not only by temperature but also by an energetic plasma formed by the electric (Direct Current or Radio Frequency) field. PECVD is generally used in situations where the substrate material or the deposited films have a low thermal tolerance and would otherwise suffer from thermal degradation if exposed to the higher temperatures caused by thermal CVD. By changing the nature of plasma, we can additionally add a controller to the properties of thin film deposition and graphene growth.

PECVD is incorporated for the fabrication of different semiconductor devices. It is also used in industrial coverings where conformism, high material density, high purity, and

uniformity are required but where the substrate material or deposited film cannot withstand high temperatures.

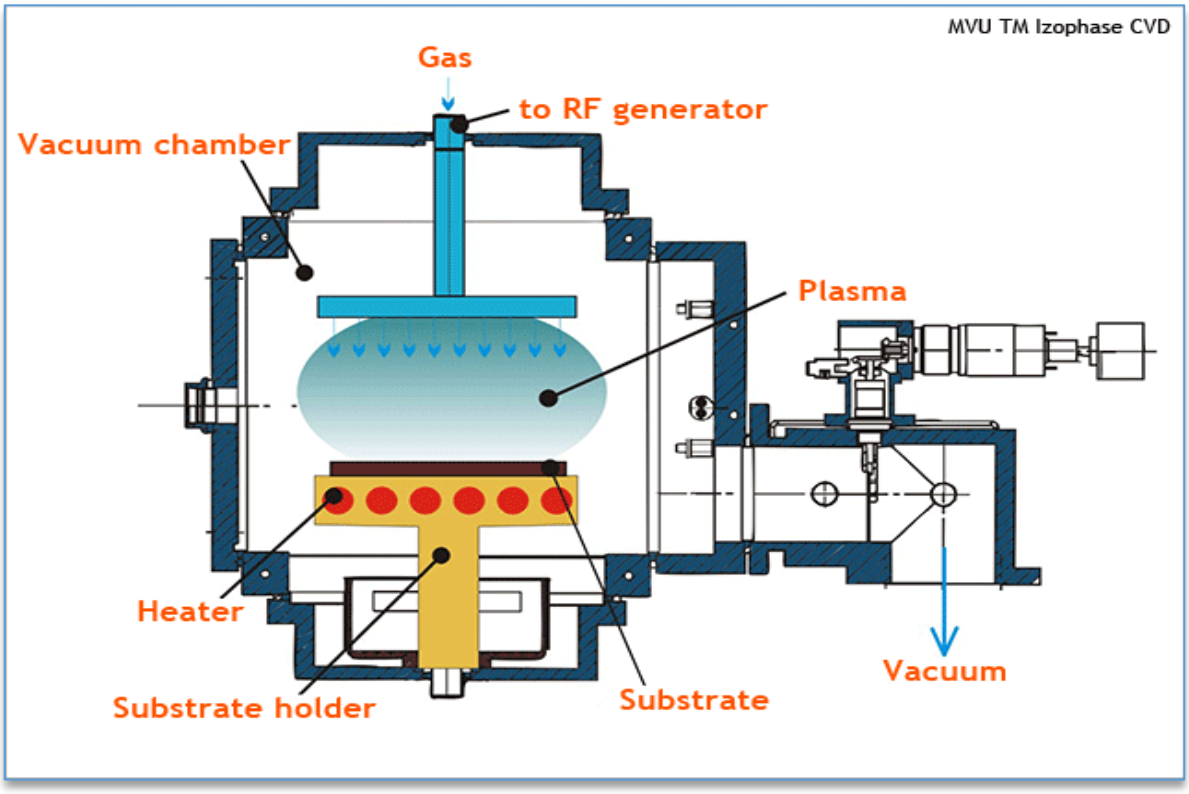

Figure 1.7 Schematic Diagram of Plasma Enhanced Chemical Vapor Deposition from MVU TZM Iozophase Ltd.

Contrasting with other CVD processes, one of the primary points of interest of PECVD is that this technique can be worked in low temperature while the deposition rate is equivalent to other CVD forms. PECVD by and large works at a low temperature in the middle of 100˚C and 400˚C. The PECVD procedure utilizes both warm vitality and RF-incited glow discharge to control the synthetic responses. The glow discharge release makes free electrons to slam into reactant gases and separate them to create the response and deposit the solid film on the substrate. Since part of the vitality to start the substance responses is provided by the glow discharge, the framework requires less thermal energy. In this way, the temperature can keep up in a relatively low-level contrasting with other CVD forms.

1.9 APPLICATIONS

Graphenes have extraordinary electrical conductivity, thermal conductivity, and mechanical properties. These amazing characteristics give graphene, great potential in numerous applications.

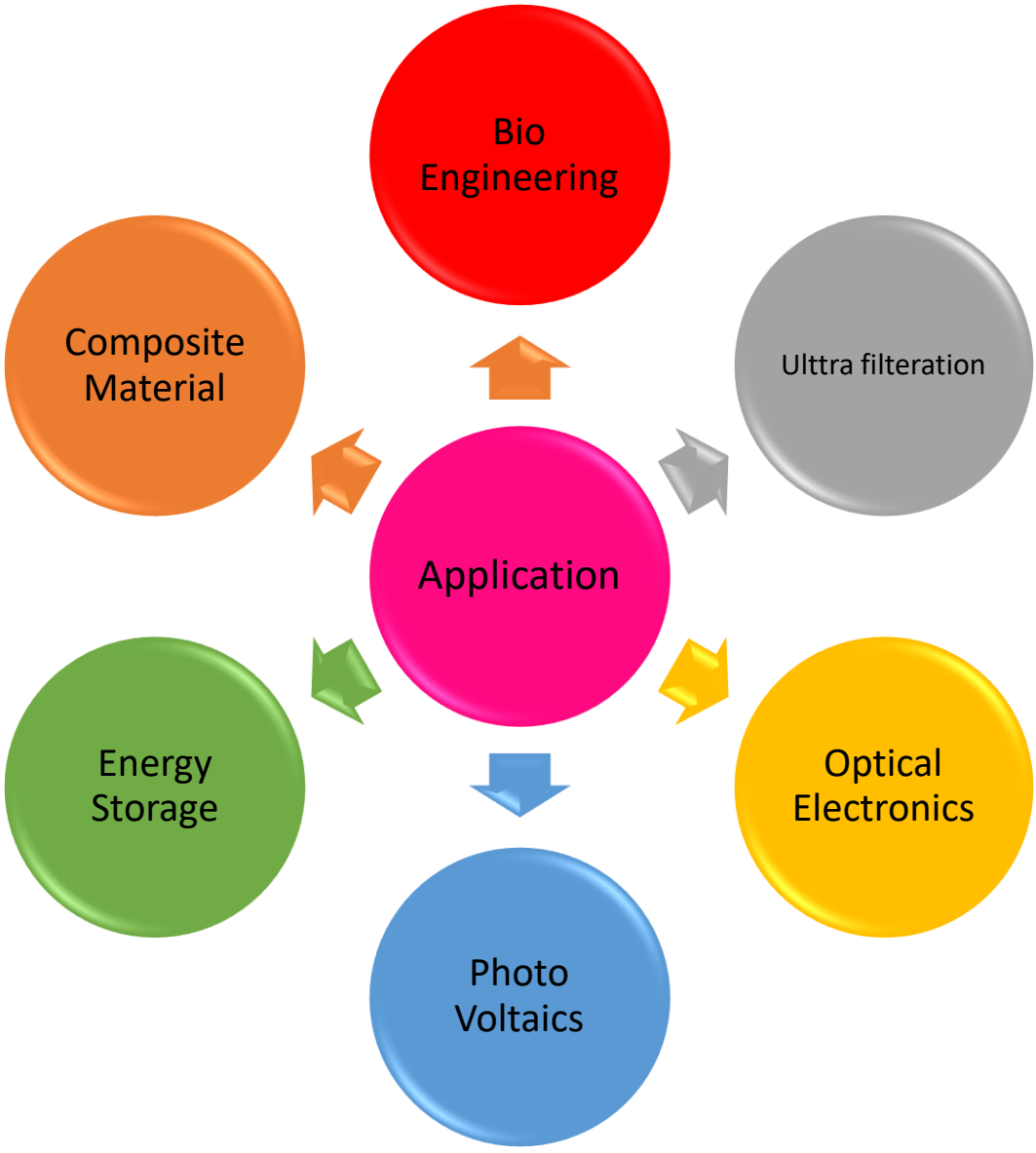

Figure 1.8 Various Applications of Graphene

1.9.1 Biological Engineering

- **Bioelectric sensory devices:** It can be used for making devices for monitoring glucose levels, hemoglobin levels, and cholesterol.
- **Anti-biotic:** Engineered toxic graphene can be implemented in biomedical as antibiotics as well as for targeted cancer treatment.
- **Tissue Regeneration:** the molecular make-up feature and biocompatibility of graphene make it suitable for tissue regeneration.

1.9.2 Optical Electronics

- **Graphene-based e-paper:** Graphene being thin and flexible structure have the ability to display interactive and updatable information on surfaces.
- **Optoelectronics:** It can be used in touchscreens technology, liquid crystal displays (LCD) and organic light emitting diodes (OLEDs) for smartphones, tablet, and desktop computers and televisions.

1.9.3 Ultrafiltration

- **Water filtration systems:** Graphene can be used in the removal of particulates and micro-organisms, as the pore size is in the range of nanometer.
- **Desalination system:** For turning abundant saline water into drinkable water.
- **More viable biofuel creation:** Graphene allows water to pass through it, it is almost completely impervious to liquids and gases, making it suitable for biofuel creation.

1.9.4 Composite Material

- **Aerospace:** Aerospace engineers are using carbon fiber into the production of advanced aircraft as it is also very strong and light.
- It could be used as a coating material for aircraft surface to prevent electrical damage resulting from lightning strikes due to its electrical conductivity.

- **Armors:** development of high strength material applications such as body armor for military personnel and vehicles etc.

1.9.5 Photovoltaic cells

- Graphene supports very low levels of absorption of light up to 2.7% of white light and also offers higher electron mobility. That means it can be incorporated as a substitute to silicon or ITO for the manufacturing of photovoltaic cells.
- Graphene being very flexible and ultra-thin means that graphene-based photovoltaic cells can be used in clothing; to help recharge your devices, or even used as photovoltaic window screens or curtains to help power your home.

1.9.6 Energy Storage

- **Supercapacitors:** Faster charging and high energy storage without compromise in any one feature
- **Lithium-Ion Batteries:** by assimilating graphene as an anode bids much higher storage capacities with higher longevity and charge rate**.**
- It can be used in higher energy usage applications such as electric powered vehicles, or they can be used as batteries in smartphones, laptops and tablet PCs but at intentionally lower size and weight.

1.10 COMSOL MULTIPHYSICS

COMSOL Multiphysics 5.2a is an exceptional cross-platform tool. It performs finite element analysis and incorporates a solver, analyzer and multiphysics simulation tool. It performs solving of partial differential equations (PDEs) involving various physics-interfaces in one package.

This simulation tool helps in mimicking and simulating the actual experimental condition by coupling various physics interfaces involved in any physical phenomenon. All the physical parameters and initial conditions are fed in COMSOL tool and based on these

parameters COMSOL solve the partial differential equations related to it and this helps in simulating the actual conditions for any time.

COMSOL comes with equation solvers which makes it easier and faster to work with. But the most astonishing part of COMSOL is the graphical interface and options for multiple physics in one package.

We can use COMSOL Multiphysics COMSOL for a combined workflow in many application areas, just a few examples being:

- Chemical reactions
- Diffusion
- Fluid dynamics
- Fuel cells and electrochemistry
- Bioscience
- Acoustics
- Electromagnetics
- Geophysics
- Heat transfer
- Micro-electromechanical systems (MEMS)
- Microwave engineering
- Optics
- Photonics
- Porous media flow
- Quantum mechanics
- Radio-frequency components
- Semiconductor devices

2

SIMULATION MODEL

In the present simulation model, the growth of graphene is studied.in $Ar/C_2H_2/H_2$ reactive plasma using COMSOL Multiphysics 5.2a modeling suite. The methodology adopted in the simulation involves four physical stages.

1) **Plasma Interface** involves the ionization of gas mixture due to the transformer action caused by the inductively coupled plasma action by RF coils. This ionization leads to electron generation followed by series of electron impact reaction.

The plasma generated leads to an increase in temperature inside the PECVD chamber. Under the effect of high temperature around the substrate, the nickel catalyst coating on the substrate changes into clusters of Nanoparticles called Islands. These islands or catalyst Nanoparticle act as adsorption sites for carbon species.

2) **Heavy Species Transport (HST)**, involves the exposure of carbon-containing gases with plasma excited species in order to produce various ions and radicals. It also involves the interaction of these fluxes with the catalyst.

In our model acetylene is the carbon-containing gas which we used for growth of graphene-like structure. Under HST this acetylene gas goes under ionic as well as thermal decomposition to dissociate into various ions and neutrals as stated in Table 2.3

3) **Magnetic Field**, plays an important role in the generation of high power radio frequency through coils to initiate ionization of gases to form the plasma by induction effect. Another module of a magnetic field is used for providing power to substrate bias coil.

Depending on the requirement of power for RF power coil and substrate bias coil, the intensity of applied magnetic field proportional to applied power ranges from 100W-1500W for RF Power Coil and 0 to -400 V DC for substrate bias coil

4) **Substrate Bias or Laminar Flow** supports the directed flow of fluxes of various carbon species towards the catalyst coated substrate.

As the fluxes of carbon-containing gas and Hydrogen gas mostly being positively charged as can be seen from Table 2.3. These ions are directed towards the negatively biased substrate. These fluxes of carbon-containing ions and neutrals go under series of adsorption, thermal decomposition, ion-induced decomposition and desorption at the catalyst Nanoparticle sites, finally leading to the growth of carbon structures.

These physical interfaces are coupled in the 2D axis symmetric geometry constructed in the Inductively Coupled Plasma (ICP) module in COMSOL Multiphysics 5.2a. We have developed a two-dimensional PECVD model of plasma of complex $Ar/C_2H_2/H_2$ gas mixtures at low-pressure 20mTorr and low temperature below 723K, which makes it convenient to grow carbon Nanostructure on the substrates that cannot withstand high temperature.

2.1 MODEL ASSUMPTIONS

The basic assumptions in the model formulation are:

(a) The actual 3D cylindrical Plasma chamber which restrict the analysis to a 2D axis-symmetric geometry for analysis purposes.

(b) Coating of Nickel as catalyst material on Silicon (100) substrate uniformly in pre-plasma conditions.

(c) The dielectrics are taken as insulators to electrically decouple plasma chamber and the coils,

(d) Operating conditions in the chamber are assumed uniform.

(e) Frequency transient study of the system is analyzed using COMSOL Multiphysics 5.2a

(f) Convection of heavy species present in a plasma can often be neglected due to the low operating pressure.

(g) The surface loss of hydrogen atoms is assumed to be zero at the boundary walls of plasma chamber.

(h) The electron emission due to ion impact is set to zero and ions are considered as completely absorbed/ neutralized when they arrive at the chamber boundary with the only transitional change in the state of Ar.

(i) The excited hydrogen atoms and argons are set to revert to their ground states when they contact with the walls.

2.2 GEOMETRY AND MATERIAL

A half 2D axis-symmetric geometry [19] of the side view of the actual Plasma Enhanced Chemical Vapor Deposition chamber was designed in COMSOL Multiphysics v5.2 (COMSOL AB, Stockholm, Sweden) as shown in Figure 2.1. The same 2D axis symmetric geometry is considered for the simulation of the various sets of operating conditions. The schematic 3D PECVD model is shown in the inset of figure 2.1, which represents the actual model.

In Figure 2.1, the plasma reactor chamber consists of a metal cylinder of radius 10 cm and height 15 cm. A substrate platform of radius 7 cm is placed 8 cm below the chamber top. A four-turn spiral antenna [19] (inductive coil) named Coil 1 is located at the top of the chamber and is connected to a 13.56 MHz generator providing power ranging from 1200 W

to 1500 W. This RF coil is the main source for ICP plasma source. The antenna configuration with only four coil turns was chosen intentionally to generate low-temperature plasmas with non-uniform density profiles along the radial direction [20]. A substrate bias named coil 2 is also provided beneath the substrate consisting of DC voltage source with biasing ranged from -10 V to -400 V DC.

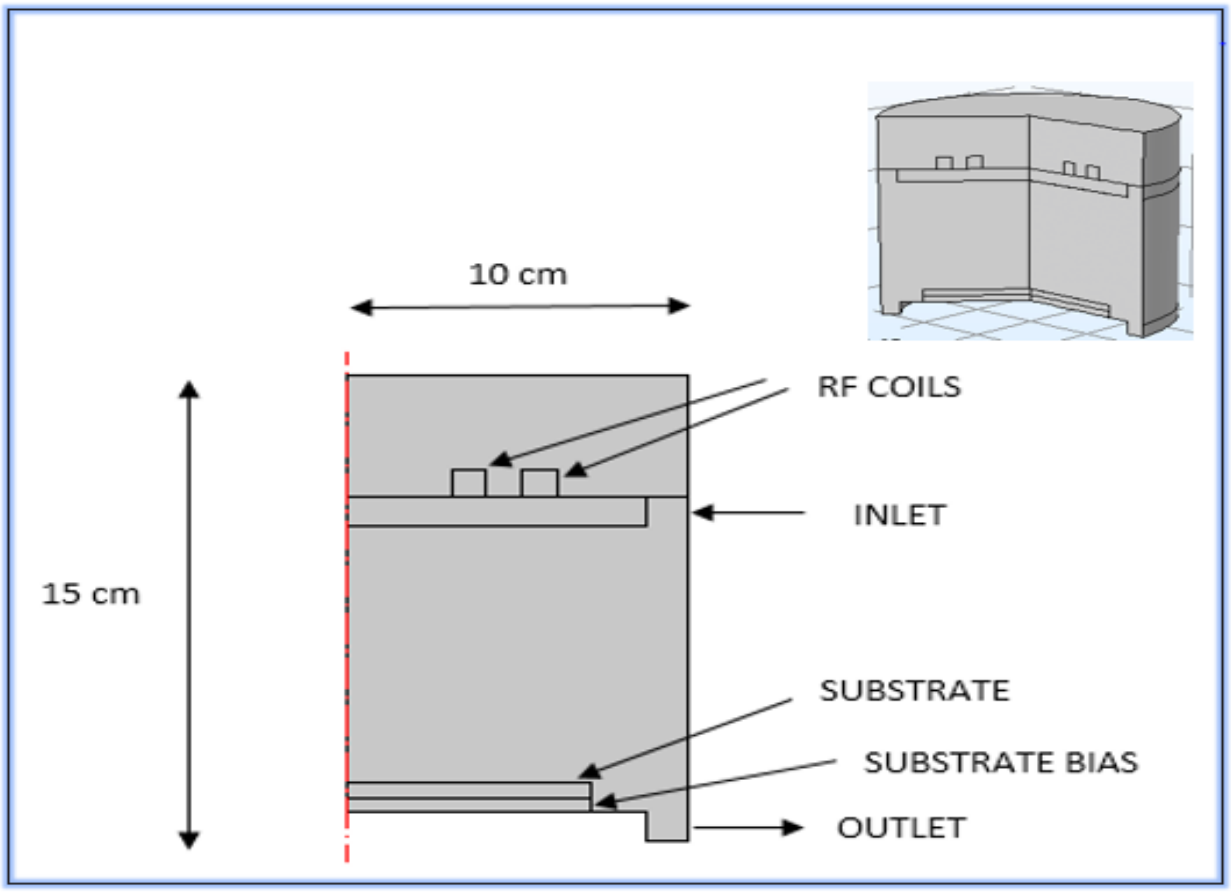

Figure 2.1 Schematic Diagram of 2D axis-symmetric PECVD model considered for simulation with actual 3D PECVD model in the inset

In Figure 2.1, the plasma reactor chamber consists of a metal cylinder of radius 10 cm and height 15 cm. A substrate platform of radius 7 cm is placed 8 cm below the chamber top. A four-turn spiral antenna [19] (inductive coil) named Coil 1 is located at the top of the chamber and is connected to a 13.56 MHz generator providing power ranging from 1200 W

to 1500 W. This RF coil is the main source for ICP plasma source. The antenna configuration with only four coil turns was chosen intentionally to generate low-temperature plasmas with non-uniform density profiles along the radial direction [20]. A substrate bias named coil 2 is also provided beneath the substrate consisting of DC voltage source with biasing ranged from -10 V to -400 V DC.

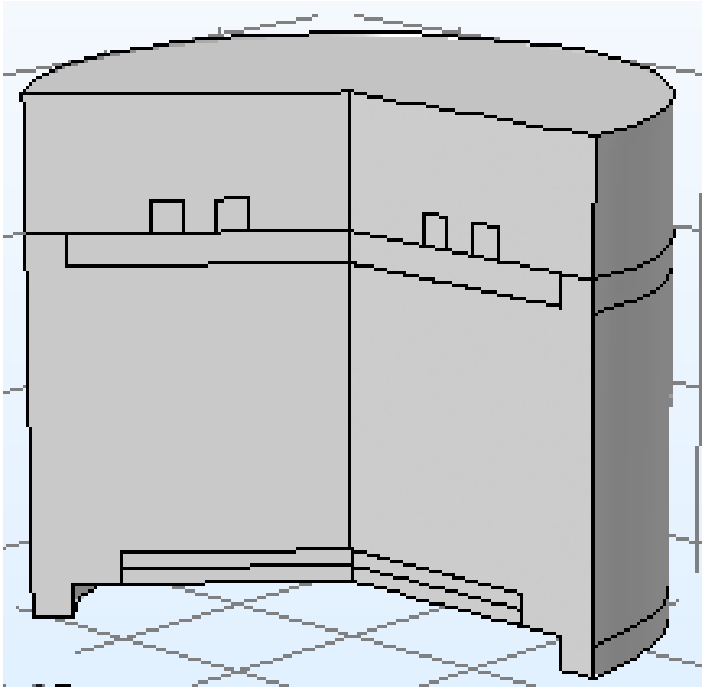

Figure 2.2 Schematic Diagram of actual 3D PECVD model

Meshing is a critical step in plasma model, which is needed to capture the separation of space charge between the electrons and ions close to the wall. Inductively coupled plasma and heavy species transport is computationally meshed using COMSOL Multiphysics v5.2a (COMSOL AB, Stockholm, Sweden). The material and spatial domains are meshed using finer boundary layer mesh based on the COMSOL physics-controlled mesh of minimum quality of 0.001m. The plasma chamber domains are meshed using extra fine element size with the free triangular entity as shown in Figure 2.2. The boundary layer property involved a total of 5 boundary layers with the stretching factor of 1.4.

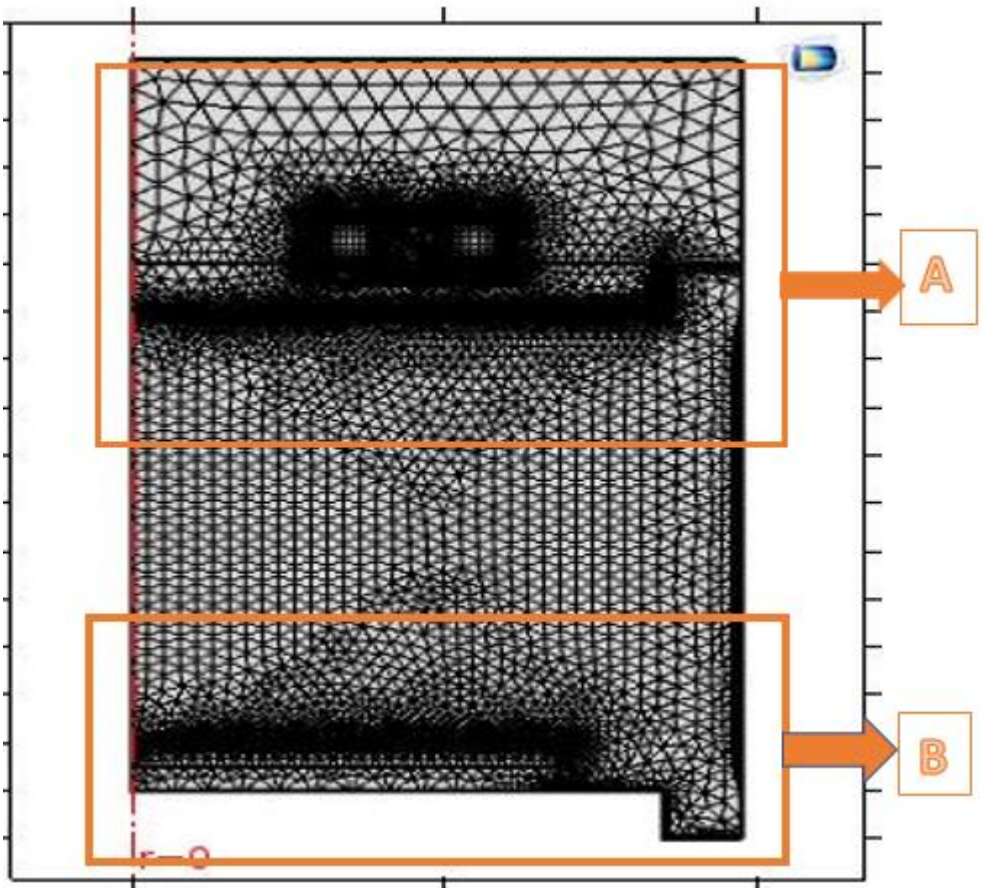

Figure 2.3 Meshing of 2D axis-symmetric PECVD Model

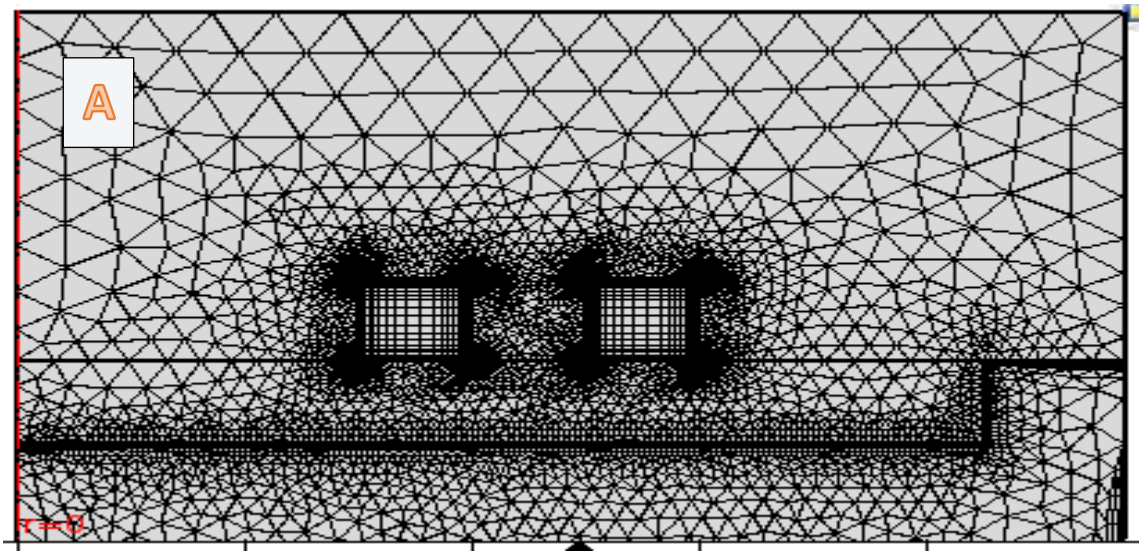

Figure 2.3.1 Meshing near Power coil and dielectric region

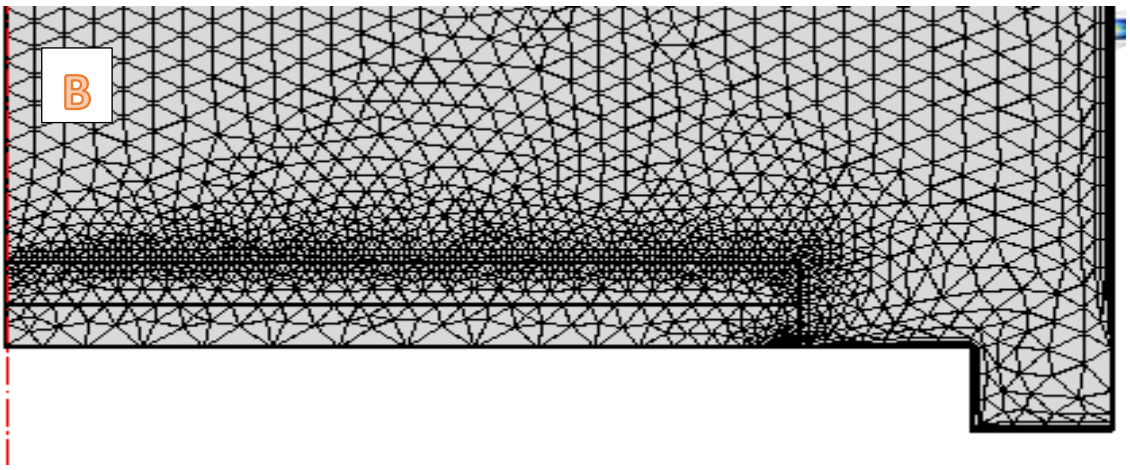

Figure 2.3.2 Meshing near the substrate and biasing coil

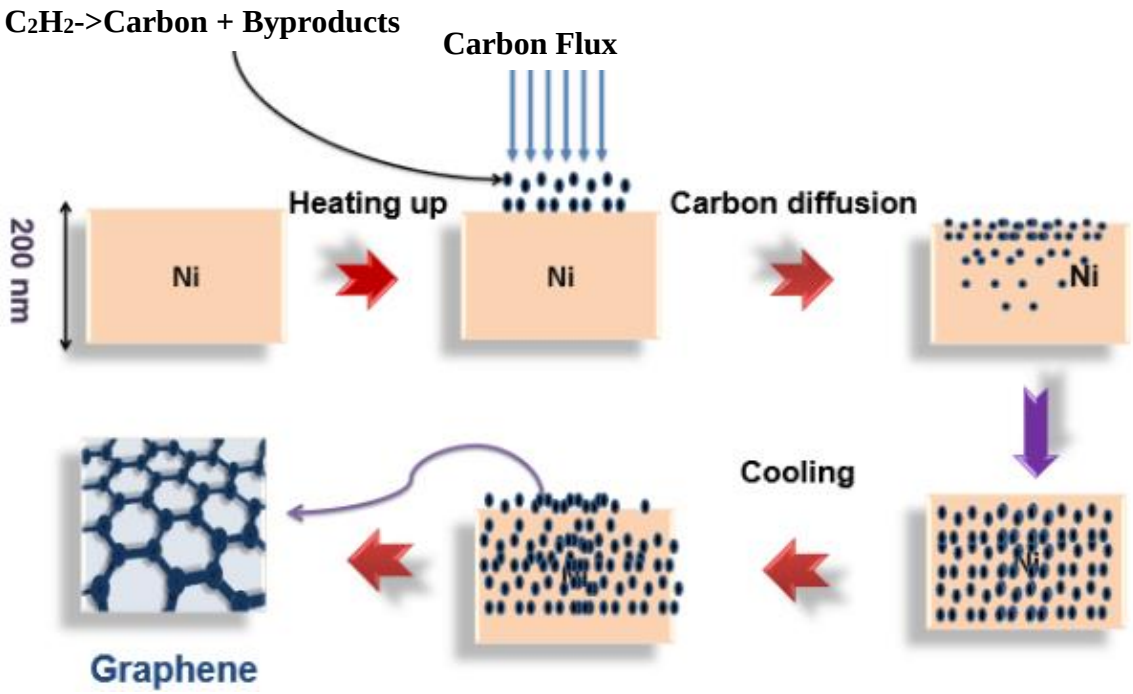

Figure 2.4 Schematic showing the mechanism for CVD graphene growth on Ni. Image by K. M. Al-Shurman and H. A. Naseem and is taken from the poster titled "CVD Graphene Growth Mechanism on Nickel Thin Films".

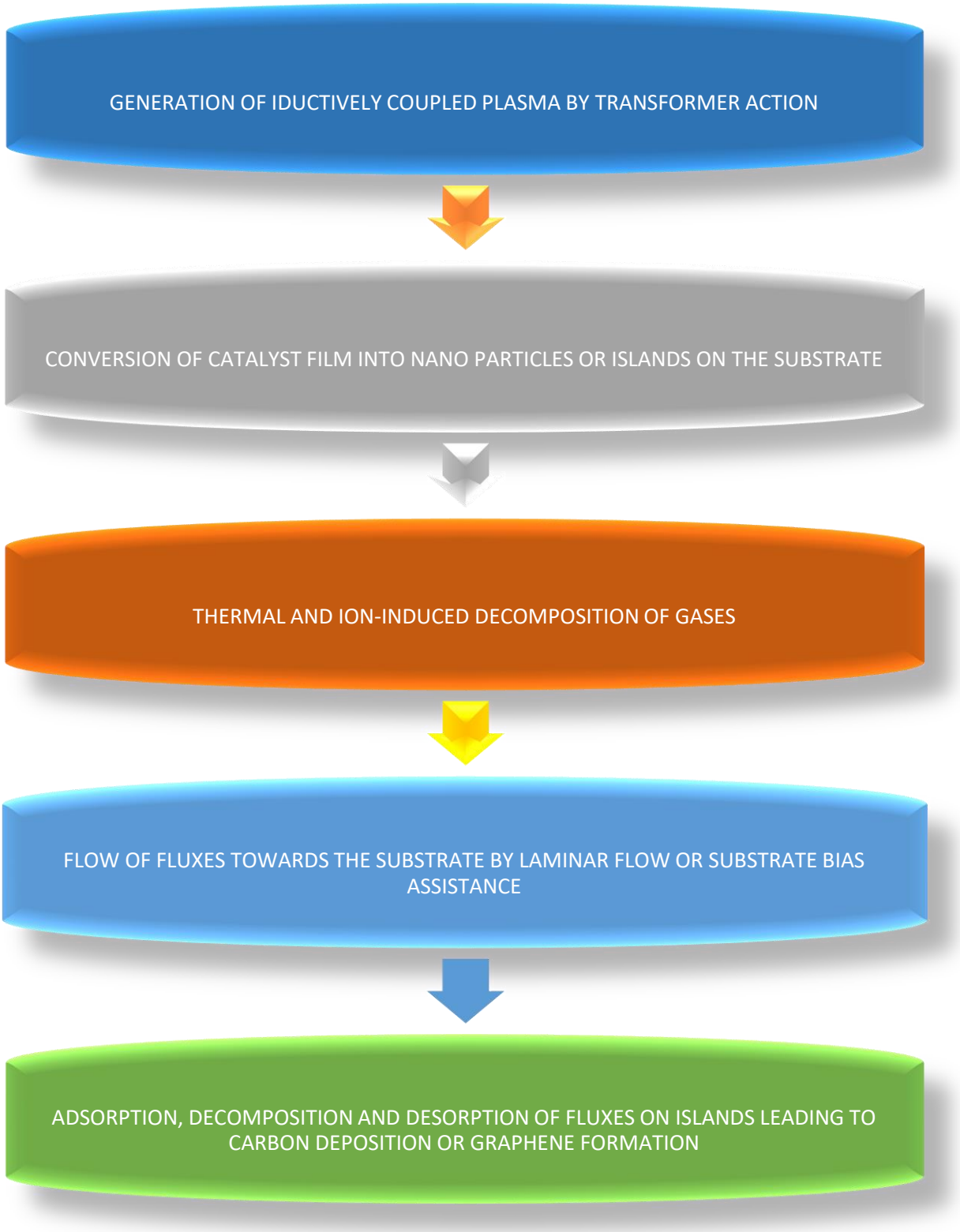

Figure 2.5 Flow chart for the mechanism of growth of carbon nanostructures by PECVD technique

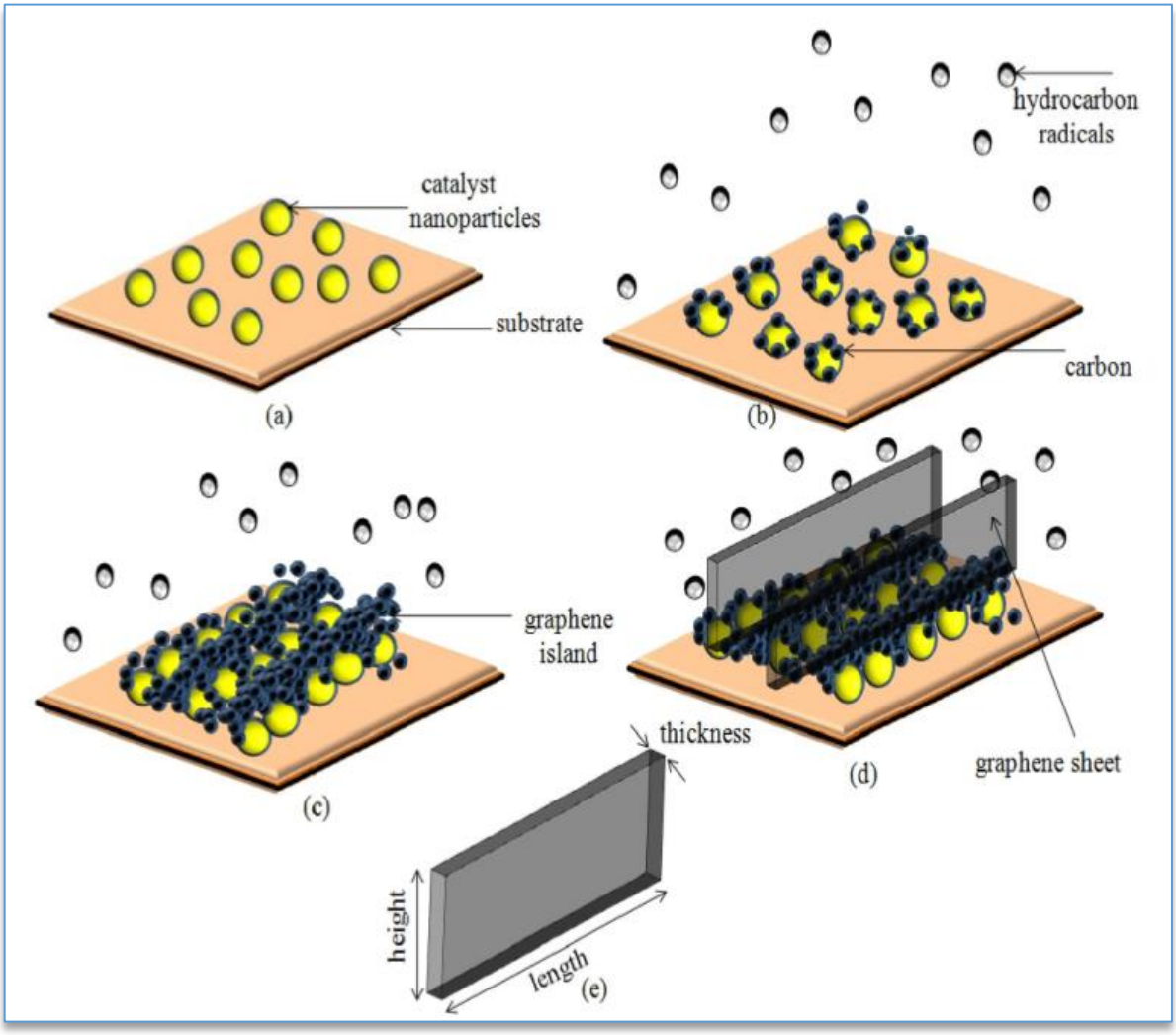

Figure 2.6 Schematic representation of the formation of graphene sheet under the plasma by Suresh C. Sharma and Neha Gupta image taken from paper titled "Theoretical modeling of the plasma-assisted catalytic growth and field emission properties of graphene sheet, Physics of Plasmas (22), 123517 (2015)"

Figure 2.5 describes the process of formation of vertical graphene nanofilms under the effect of plasma. The process encompasses the creation of catalyst nano-particles over the substrate surface followed by formation of clusters due to the dispersion of carbon atoms on the catalyst nanoparticles. Later on, the diffusion of these clusters leads to the development of islands of graphene on the substrate surface.

At the boundaries of these graphene islands growth of vertical graphene sheets takes place, due to the effect of tensile stress generated at the edges and also due to the effect of the charged plasma sheath.

Table 2.1 Materials used for various Domains

Medium	Electrical Conductivity	Relative Permittivity	Relative Permeability
RF coils (Coil 1)	$6x10^7$ S/m	1	1
Substrate Bias (Coil 2)	$4x10^3$ S/m	1	1
Dielectrics/Insulators	0	1	4.2

Table 2.2 Plasma Parameters

Parameters	**Value**
Input Plasma Power	1200 (W)
Gas Pressure	20 (mTorr)
Gas Temperature	300 & 723 (K)
Reduced Electron Mobility	$4x10^{24}$ (1/V.m.s)
Area of the substrate	154 cm^2
Thickness of Nickel Coating	200 nm
Initial Electron Density	10^{13} ($1/m^3$)
Plasma Power frequency	13.56 MHz (Radiofrequency)

Table 2.3 Different species considered in the Ar/C2H2/H2 model, besides electrons

Molecules	Ions	Radicals	Surface Species
Ar	Ar+, ArH+	Ars	
C2H2	C_2H+, C_2H+, C_2H_3+	C_2H, C_2H_3	C_2H_2(s), C_2H(s), C(b)
H2	H+, H_2+, H_3+	H	H(s), H_2(s), H(b)

In this Simulation, the numerical modeling of reactive CVD process is carried out using COMSOL. The model involves the solution of multiple plasma and surface reaction equations for a number of reactants and intermediate species. These reaction equations are provided with tens of finite rate reaction steps and varying rate coefficients. The solution of such rigid sets of equations is difficult and the inbuilt solver of COMSOL does the job accurately and very fast. COMSOL has an easy to use GUI and different inbuilt equation solver of COMSOL provided with various Multiphysics options.

2.3 PHYSICS AND EQUATIONS INVOLVED

The model incorporates following physics interfaces:

Plasma Interface

Under Plasma physics section of COMSOL as plasma source where the energy is supplied by the electric current which is produced by electromagnetic induction, that is a time-varying magnetic field.

When a time-varying electric current is supplied to the RF coils at 13.56 MHz, it produces a time-varying magnetic field in the plasma chamber filled with gases. As per Lenz's law, a time-varying electric current flows inside the chamber gases in opposite direction to oppose the magnetic field. This electric current in the gas chamber ionizes the Argon gas to form the plasma by transformer action.

The Plasma interface, found under the Plasma couples the Drift-Diffusion, Heavy Species Transport, and magnetic field interfaces into an integrated Multiphysics interface to model inductively coupled plasmas.

Heavy species Transport

The Heavy Species Transport interface is a mass balance interface for all non-electron species formed in the plasma chamber. This physics interface also makes it possible to add electron impact reactions, chemical reactions, surface reactions, and species, including charged, neutral, and electronically excited species into the model to simulate the actual reactions taking place experimentally.

The electron transport properties are computed from the reduced transport properties using equation $\mu_e = \frac{\mu_{red}}{N_n}$ (1)

where N_n is the user-defined neutral number density and μ_{red} is reduced mobility of electron.

The Cross-section data is used to define source coefficients in the model, here the Maxwellian electron energy distribution function (EEDF) is used to define source coefficients $f(\varepsilon) = \varphi^{-\frac{3}{2}}\beta_1 \exp(-(\frac{\varepsilon\beta_2}{\varphi}))$ (2) where $\beta_1 = \Gamma(\frac{5}{2})^{\frac{3}{2}}\Gamma(\frac{3}{2})^{-\frac{5}{2}}$, $\beta_2 = \Gamma(\frac{5}{2})\Gamma(\frac{3}{2})^{-1}$, φ is the mean electron energy (SI unit: eV), ε is the electron energy (SI unit: eV) and Γ is the incomplete gamma function.

Electron Transport

COMSOL Multiphysics solves a pair of drift-diffusion equation 3 &4 for the electron density and electron energy density respectively

$$\frac{\partial}{\partial t}(n_e) + \nabla.\Gamma_e = \mathrm{R_e} \quad (3)$$

$$\frac{\partial}{\partial t}(n_e) + \nabla.\Gamma_e + E.\Gamma_e = \mathrm{R_e} \quad (4)$$

$$\Gamma_e = -n_e(\mu_e E) - D_e \nabla n_e \quad (5)$$

$$\mathrm{R_e} = \sum_{i=1}^{M} X_i K_i N_n n_e \quad (6)$$

$\mathrm{R_e}$ is the source term given by equation6, where K_i the rate coefficient is, N_n the number density of reactants, E is the electric field in the chamber and n_e is the electron density.

Electrostatic Potential

The plasma potential is computed from Poisson's equation $-\nabla.\varepsilon_o\varepsilon_r\nabla V = \rho$. The space charge density ρ is computed from the number densities of electrons and other charged species by equation 7.

$$\rho = q(\sum_{k=1}^{M} Z_k n_k - n_e) \quad (7)$$

Surface Reaction

Surface reactions can be specified in terms of rate or sticking coefficients. The surface rate constant is determined using equation 8.

$$K_{f,i} = (\frac{\gamma_i}{1 - \gamma_i/2}) \frac{1}{(\Gamma_{tot})^m} \sqrt{\frac{RT}{2\pi M}} \quad (8)$$

γ_i is the sticking coefficient given by $\gamma_i = a_1 T^{b1} \exp(-\frac{e_i}{RT})$, where M is the mass of species, R is the gas constant, T is the temperature and a_1 and b_1 are constants.

Accumulated Carbon Growth

In this model, the precipitated carbon atoms cause a movement across direction parallel to the interface Ni film domain. So, the mass flux across the substrate divided by the density of carbon atoms being precipitated gives the rate at which the interface is moving. Hence, the velocity of the interface can be mathematically expressed by the equation $\gamma_i = a_1 T^{b1} \exp(-\frac{e_i}{RT})$. Where v_y is the interface velocity and $\vec{j}_m . n_y$ is the mass flux in y-direction and density of carbon is 2.267 g/cm^3.

Hence, the thickness (d) of the segregated carbon material can be calculated by equation d= v_y *t, where t is time.

2.4 REACTIONS CONSIDERED

The simulations are performed for the case of Ar/C_2H_2/H_2 plasma discharges operating at an RF frequency of 13.56 MHz. The RF-applied power is 1200 W. The gas pressure is 20 mTorr and the gas temperature is assumed to be 723K. The species taken into account are electrons, molecules (Ar, C_2H_2, H_2), ions (Ar^+, H^+, H_2^+, H_3+, ArH^+, $C_2H_2^+$, C_2H^+, $C_2H_3^+$), and neutrals (Ar*, H, H_2, C_2H, C_2H_3, C(b), C_2H_2(ads), C_2H(ads), H(s), H_2(s), H(b)) as shown

in Table 2. The reactions of electron impact collision and those of ions and neutral species are listed in Table 3.

Table 2.4 Reactions Involved

Electron Impact reactions				
No	Reaction	Type	Threshold(eV)	Ref.
1	$e^- + Ar \rightarrow e^- + Ar$	Elastic	0	22,23
2	$e^- + Ar \rightarrow e^- + Ars$	Excitation	11.5	22,23
3	$e^- + Ars \rightarrow e^- + Ar$	Superelastic	-11.5	22,23
4	$e^- + Ar \rightarrow 2e^- + Ar^+$	Ionization	15.8	22,23
5	$e^- + Ars \rightarrow 2e^- + Ar^+$	Ionization	4.24	22,23
6	$Ars + Ars \rightarrow e^- + Ar + Ar^+$	Penning Ionization	-	22,23
7	$Ars + Ar \rightarrow Ar + Ar$	Metastable quenching	-	22,23
Plasma chamber Wall Surface reaction				
No	Reaction	Sticking Coefficient		Ref.
8	$Ars \rightarrow Ar$	1		23
9	$Ars^+ \rightarrow Ar$	1		23
Reactions				
No	Reaction	Rate Coefficients (m^3/(s.mol))		Ref.
10	$Ar^+ + C_2H_2 \rightarrow C_2H_2^+ + Ar$	25.29 x10^8		24
11	$Ar^+ + H_2 \rightarrow Ar + H_2^+$	0.448 x10^8		24
12	$C_2H_2^+ + H_2 \rightarrow C_2H_3^+ + H$	0.1656 x10^6		24
13	$H_2^+ + H \rightarrow H^+ + H_2$	1.062 x10^7		24
14	$C_2H_2 + H^+ \rightarrow C_2H^+ + H_2$	0.713 x10^8		24
15	$C_2H_3^+ + H \rightarrow C_2H_2^+ + H_2$	1.126 x10^6		24
16	$C_2H^+ + H_2 \rightarrow C_2H_2^+ + H$	0.182 x10^8		24
17	$C_2H_2^+ + H^+ \rightarrow C_2H_2^+ + H_2$	0.713x10^8		24

Surface Reactions on the substrate				
No	Reaction	Type	Sticking Coefficient	Ref.
18	$C_2H^+ \rightarrow 2C(b)+H_2$	Dissociation of hydrocarbon	1	25-29
19	$C_2H^+ \rightarrow C_2H$	Stabilization of ions	0.8	25-29
20	$C_2H_2 \rightarrow C_2H_2(ads)$	Adsorption of Hydrocarbon on the catalyst surface	0.5	25-29
21	$C_2H \rightarrow C_2H(ads)$		0.8	25-29
22	$H \rightarrow H(ads)$	Hydrogen Adsorption on the catalyst surface	0.01	25-29
23	$H_2 \rightarrow H_2(ads)$		0.02	25-29
24	$C_2H^+ + C_2H(ads) \rightarrow 2C(b)+H(b)+C_2H^+$	Generation of Hydrogen due to ion-induced decomposition of Hydrocarbon	0.9	25-29
25	$C_2H2^+ + C_2H(ads) \rightarrow 2C(b)+H(b)+C_2H_2^+$		0.9	25-29
26	$C_2H_2^+ + C_2H_2(ads) \rightarrow 2C(b)+H_2+C_2H_2^+$		0.9	25-29
27	$C_2H_2(ads) \rightarrow 2C(b)+2H$	Thermal dissociation of Hydrocarbon	1	25-29
28	$C_2H(ads) \rightarrow 2C(b)+H$		1	25-29
29	$C_2H2^+ + C_2H_2(ads) \rightarrow 2C(b)+H+C_2H_2^+$	Ion induced dissociation of Hydrocarbon	0.9	25-29
30	$C_2H^+ + C_2H_2(ads) \rightarrow 2C(b)+H+C_2H^+$		0.9	25-29
31	$C_2H_2(ads)+H \rightarrow C_2H_3$	Loss of hydrocarbon at interaction with atomic Hydrogen from Plasma	0.3	25-29
32	$C_2H(ads)+H \rightarrow C_2H_2$		0.5	25-29
33	$C_2H_2(ads) \rightarrow C_2H_2$	Desorption of hydrocarbon	0.5	25-29
34	$C_2H(ads) \rightarrow C_2H$		0.8	25-29

The species and chemical reactions considered in the simulation are justified in order to generate 2D analysis of the number densities and fluxes of various species involved, which are vital for Nano assembly of selected carbon-based nanostructures, also to incorporate the essential channels of creation and destruction/sink of such species, and economically and time-based, stay within a reasonable computational cost. For this reason, higher hydrocarbons and other complex radical species were not included in the simulation.

3

RESULTS AND DISCUSSIONS

3.1 PLASMA CHEMISTRY AND SURFACE PHENOMENON

The average volume number densities of various plasma components including radicals, ions, and neutrals define the surface interaction with the catalyst coated substrate. The dominant plasma species comprises of Ar^+, C_2H^+, $C_2H_2^+$, $C_2H_3^+$, and H_2 at both the temperatures as seen in Figure 3.4.1 & 3.4.2. These dominant carbon-containing species mostly being positively charged are electrically attracted towards the negatively biased substrate leading to interaction with surface catalyst particles.

After activation of gaseous sources of plasma, the carbon-containing gas dissociates into constituent radicals and neutrals which later interacts with catalyst surface. Figure 3.1.1 and 3.1.2 shows the number density of C_2H^+ ion along the substrate. The density of C_2H^+ is found to be low at substrate contact point with increasing concentration outwards due to the generation of hydrogen and C_2H^+ by ion-induced decomposition of the hydrocarbon.

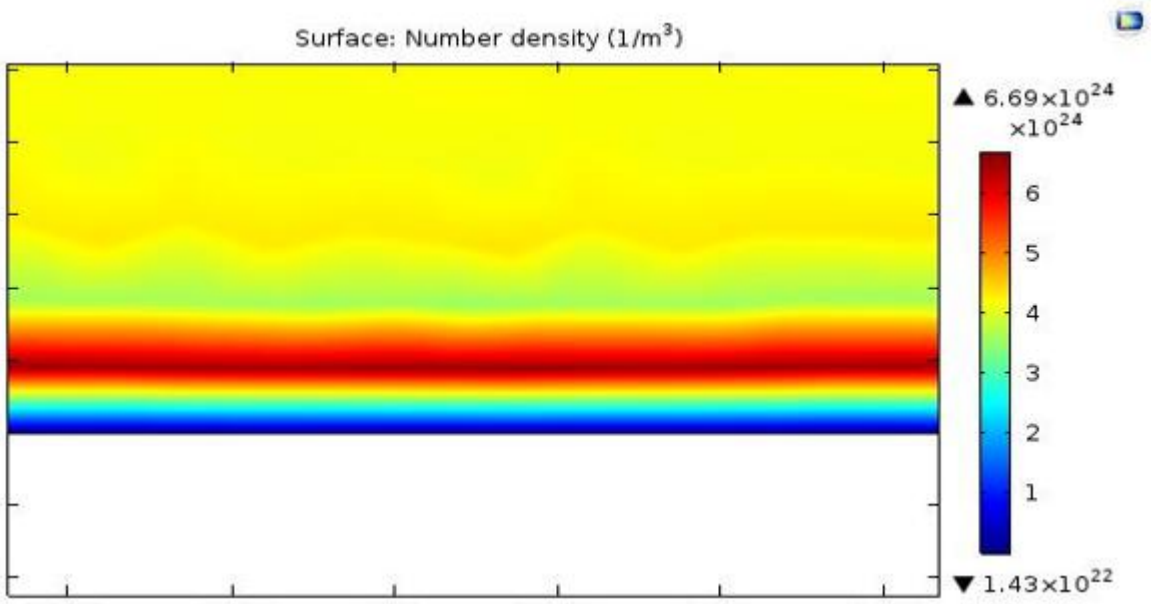

Figure 3.1.1 C_2H Number Density at 300K

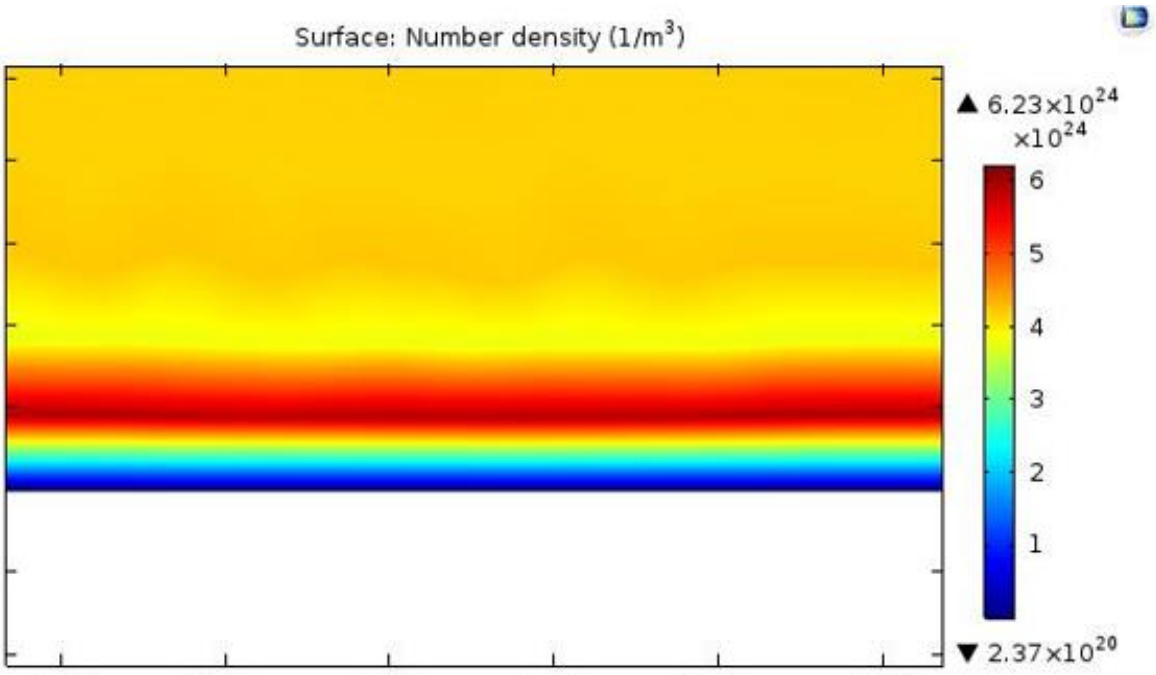

Figure 3.1.2: C_2H Number Density at 723K

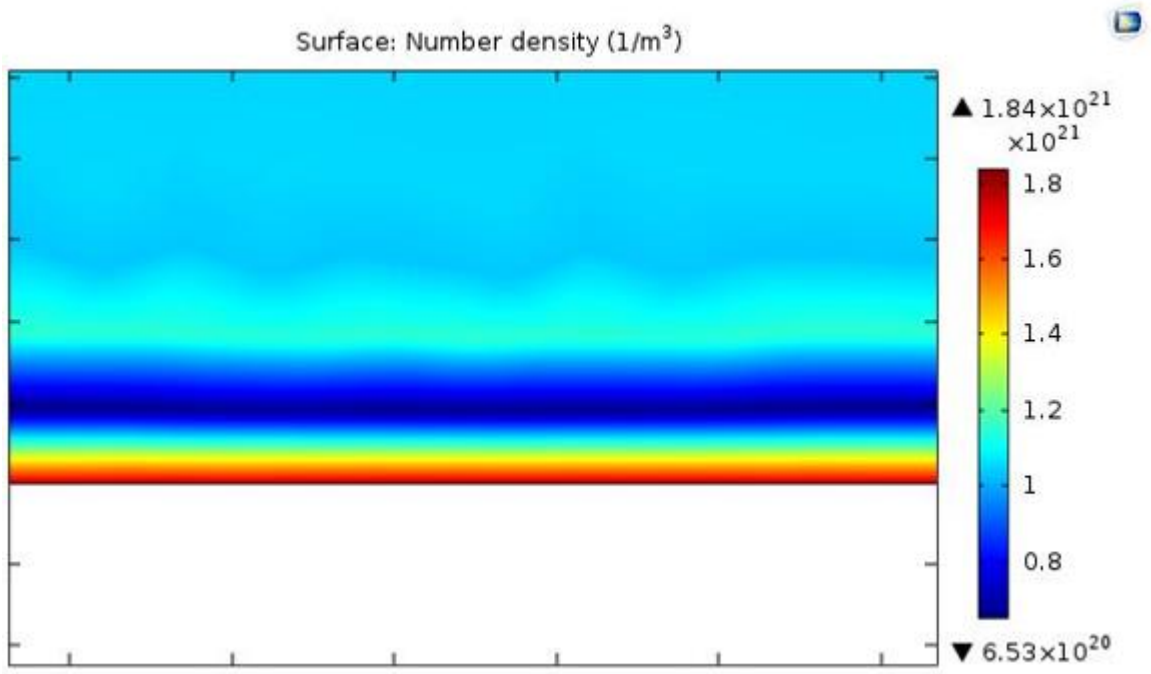

Figure 3.2.1 C_2H_2 Ion Density at 300K

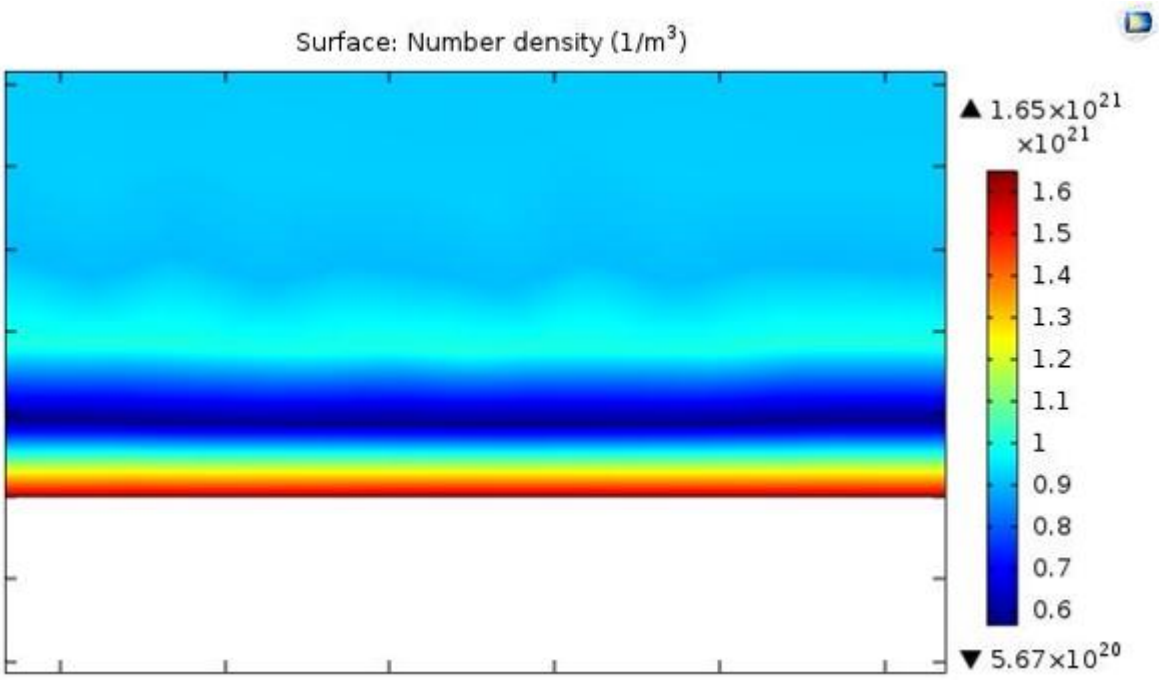

Figure 3.2.2 C_2H_2 Ion Density at 723K

Figure 3.2.1 and 3.2.2 shows the number density of $C_2H_2^+$ ion along the substrate. The density of $C_2H_2^+$ is observed to be low compared to C_2H^+ due to the low intensity of dissociation of a much heavier $C_2H_2^+$ ion.

It is found that density is higher at substrate contact point with decreasing concentration outwards because the rate of absorption of $C_2H_2^+$ is higher than the rate of desorption generation after ion induced decomposition of the hydrocarbon.

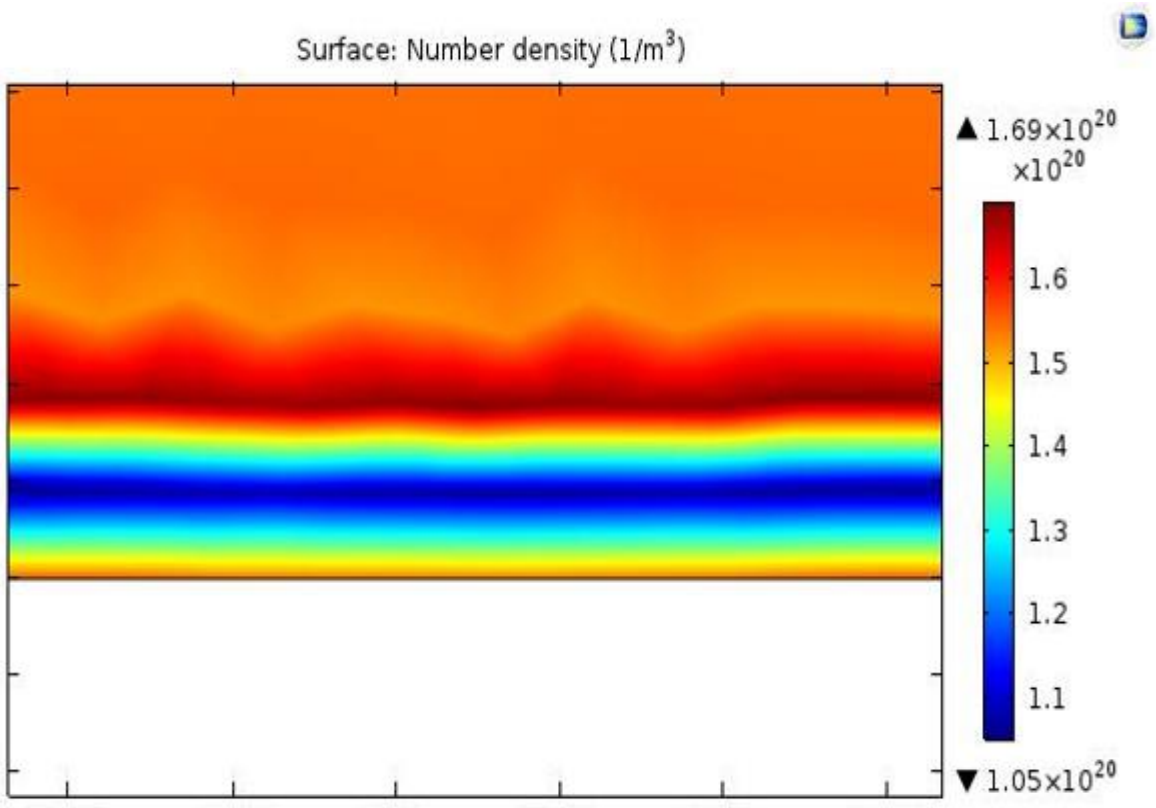

Figure 3.3.1 C_2H_3 Ion Density at 300K

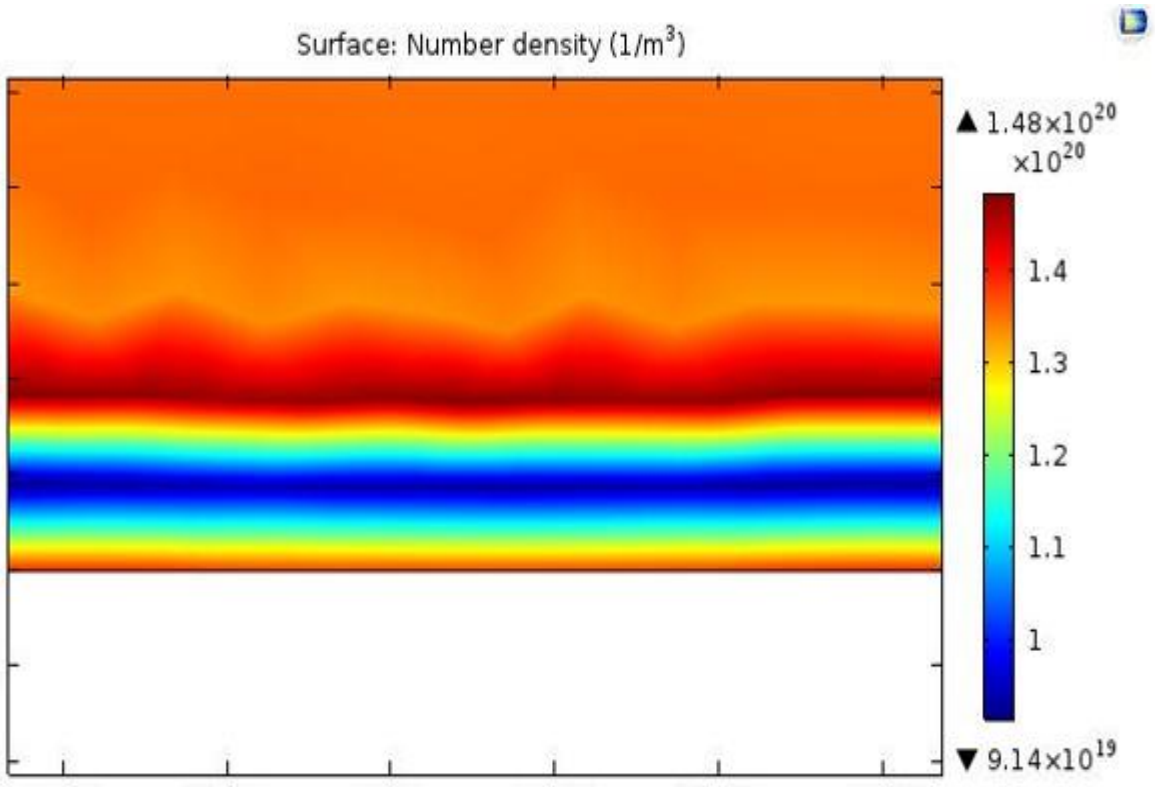

Figure 3.3.2 C_2H_3 Ion Density at 723K

Figure 3.3.1 and 3.3.2 shows the $C_2H_3^+$ ion density in the chamber along the substrate surface. It follows the same pattern as C_2H^+ with the lowest density at substrate contact and increasing density outwards but due to loss of hydrocarbon at catalyst site because of atomic hydrogens at the substrate.

The overall effect of temperature on final densities of ion and neutral species can be deduced from Figure 3.4.1 and 3.4.2 respectively. It can be inferred from the bar graph that the Ion densities of various ionic component decreased with an increase in temperature as the fraction of molecules decreases with an increase in temperature as per collision theory [30].

But, the neutral number density bar graph shows that density of neutrals C_2H_2 and C_2H_3 increased with an increase in temperature as loss of hydrocarbon from adsorbed state to gaseous state on interaction with atomic hydrogen from plasma increases.

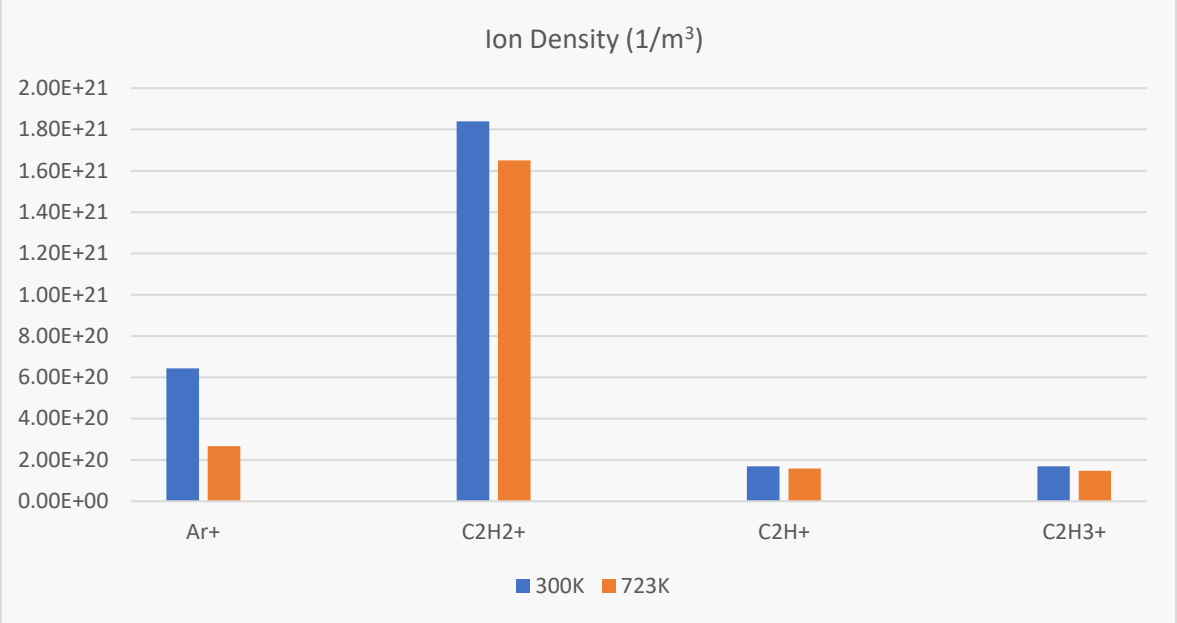

Figure 3.4.1 Number Densities of Various Ions at 300 k and 723 K

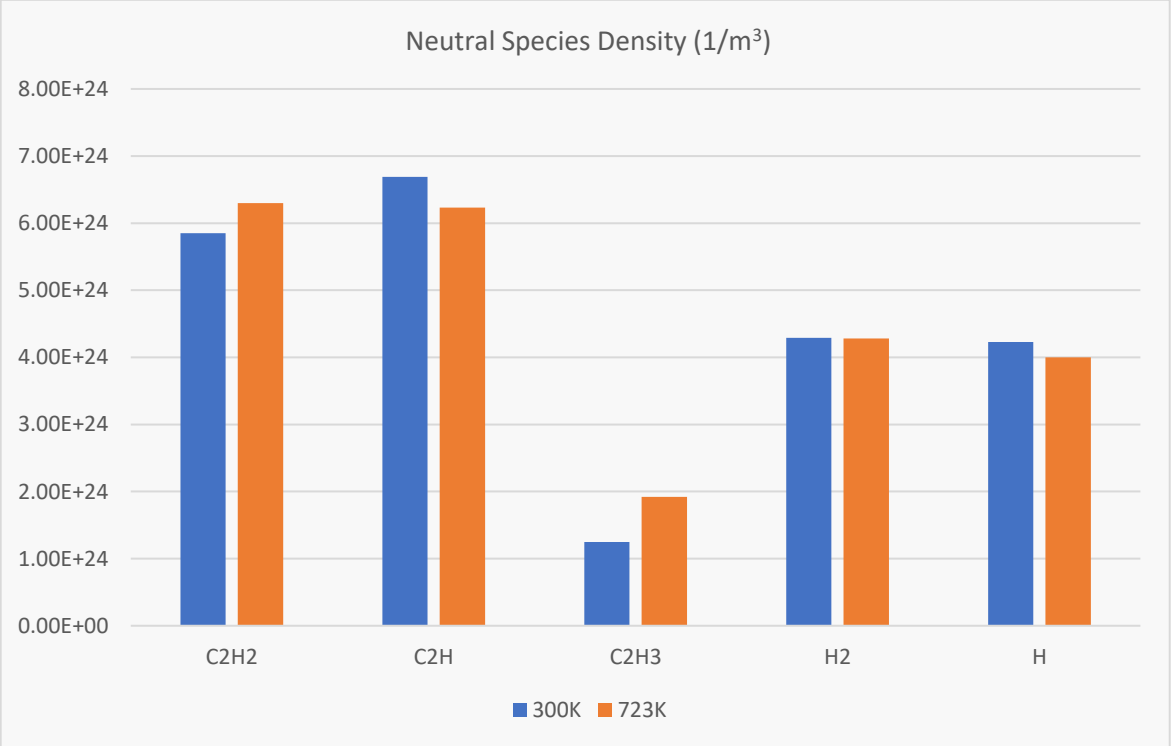

Figure 3.4.2 Number Densities of various neutral species at 300 K and 723 K

3.2 ACCUMULATED CARBON GROWTH ON THE SUBSTRATE

3.2.1) VARYING SUBSTRATE BIAS

Accumulated Carbon Growth Height

The comparison of Carbon growth and growth rate in ICP plasma generated via $Ar/C_2H_2/H_2$ at a fixed temperature is highly dependent on the substrate biasing. Figure 3.5.1 and Figure 3.5.2 shows the accumulated carbon height at a bias voltage of -50V and in absence of bias respectively at 723 K.

It can be seen that the deposition of carbon was found to be non-uniform, varying from 48-60 nm along the substrate surface. Whereas, at the edges, vertical growth was observed. The height of this vertical carbon nanostructure was found to be 223nm. On changing bias voltage, substrate carbon deposition and vertical carbon growth at the edges was observed to be in the range 340-400 nm and 660 nm respectively.

.

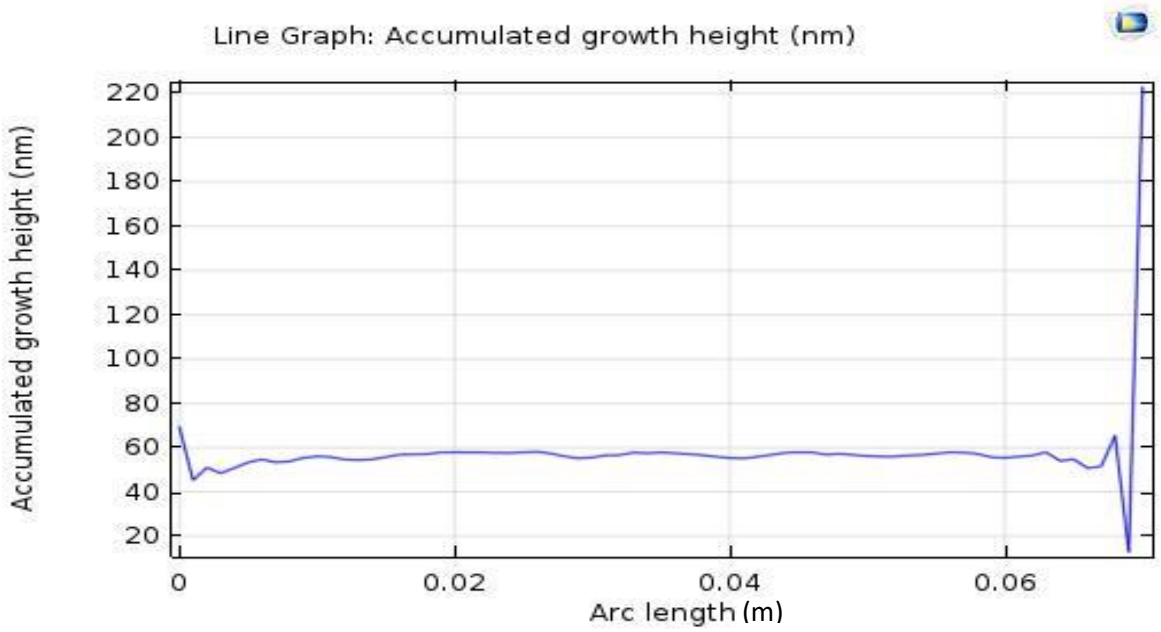

Figure 3.5.1 Accumulated carbon growth height -50 V DC bias at 723K

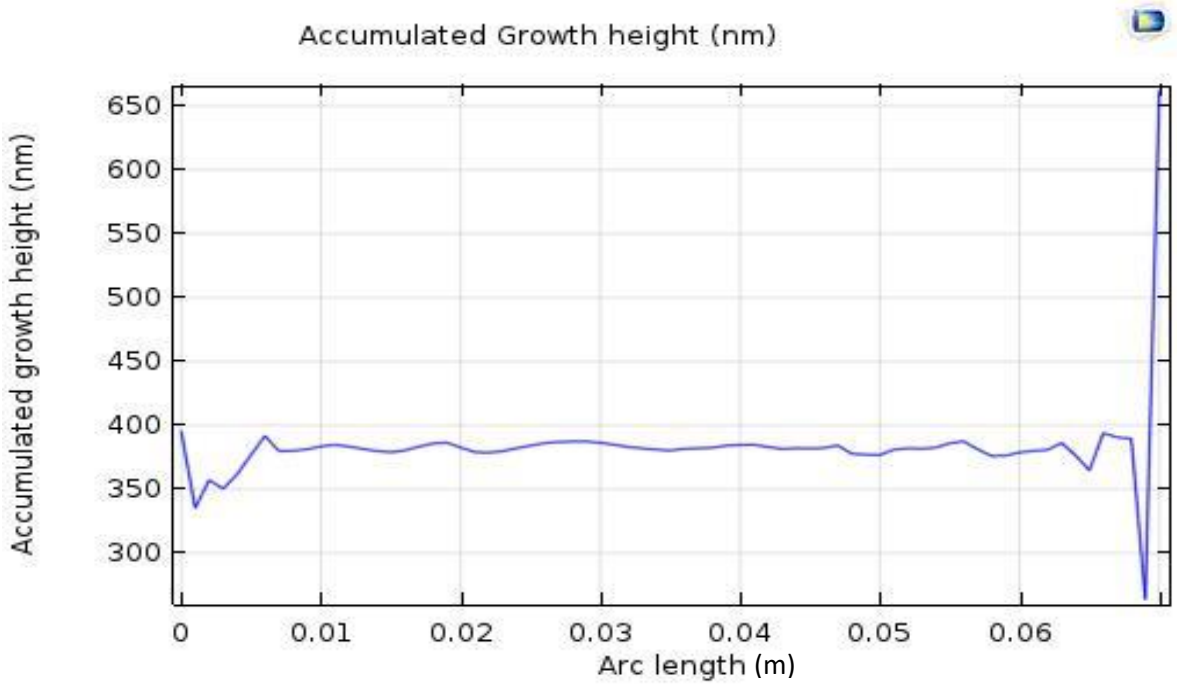

Figure 3.5.2 Accumulated carbon growth height without bias and 723K

Accumulated Carbon Deposition 3D

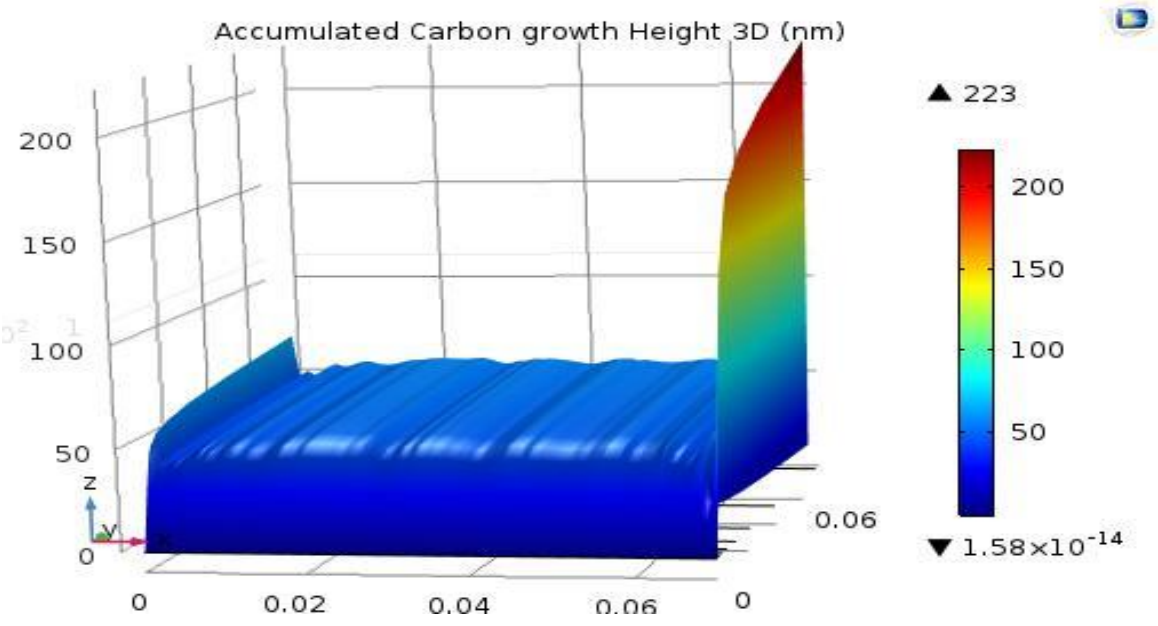

Figure 3.6.1 Accumulated carbon growth 3D at -50V DC bias at 723K

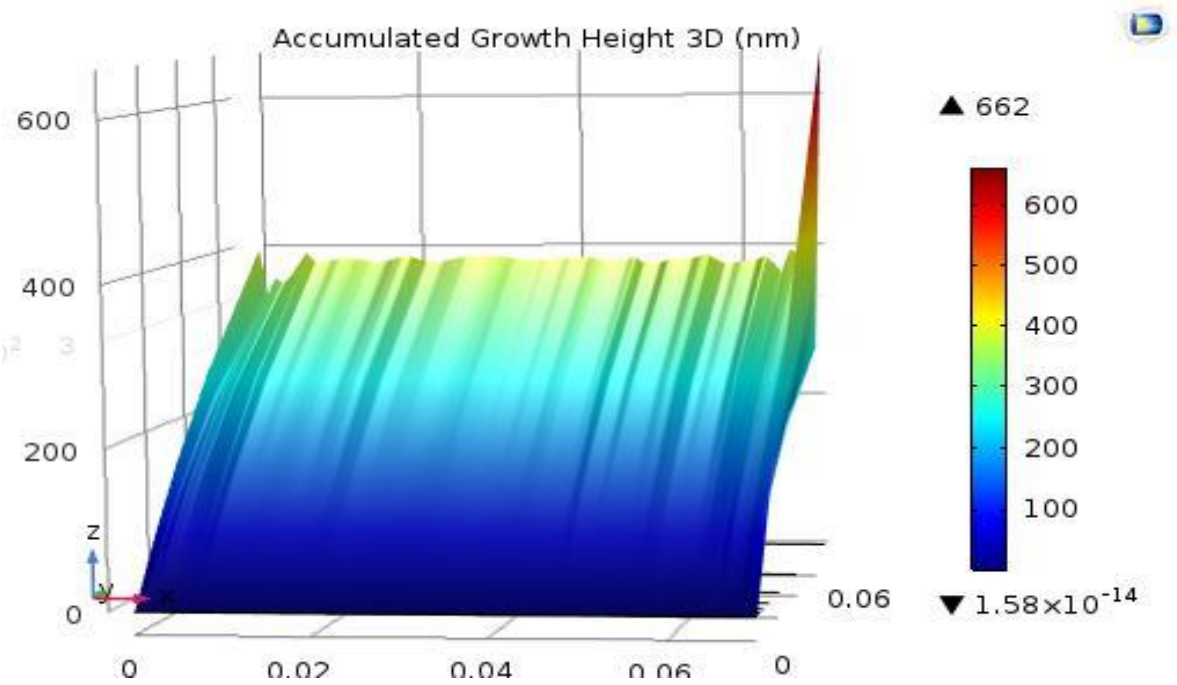

Figure 3.6.2 Accumulated carbon growth 3D without bias at 723K

Figure 3.6.1 and Figure 3.6.3 shows the 3D accumulated carbon growth on the substrate at -50V DC bias and no bias respectively There is a significant 8 fold decrease in carbon growth height on a substrate which makes it suitable for thin film deposition on desired materials.

The thickness of the horizontal graphene sheet decreases on applying to bias, because of the effective etching of the energetic ion at the sheet [32, 33]. In the absence of biasing the flux of the energetic ions towards the substrate due to which the effective etching is reduced [34]. Also, the thickness of the sheet is non-uniform due to the non-uniform flux of species as can be seen from figures 3.4.1 and 3.4.2.

At the edges of the substrate, vertical growth of sheet began due to the tensile stress developed at the boundaries. Due to the combined effect of tensile stress and alignment force exerted by plasma sheath electric field, vertical growth began [34].

Accumulated Carbon Growth Rate along the substrate arc length

The carbon growth rate along the different part of the substrate is not same in both the cases of bias and no bias as shown in Figure 3.7.1 and Figure 3.7.2 respectively One significance of providing bias is an almost uniform growth rate of carbon along the substrate horizontally except at the edge. But in case of no bias, there is a variable rate of carbon growth along the substrate.

From Figure 3.7.1 and 3.7.2 the growth rate is found to be maximum in case of no bias at around $2.2x10^{-4}$ m/s to $2.6x10^{-4}$ m/s along substrate and $6x10^{-4}$ m/s at the edge and a constant growth rate of $5x10^{-6}$ m/s along substrate and 55 $x10^{-6}$ m/s at the edge.

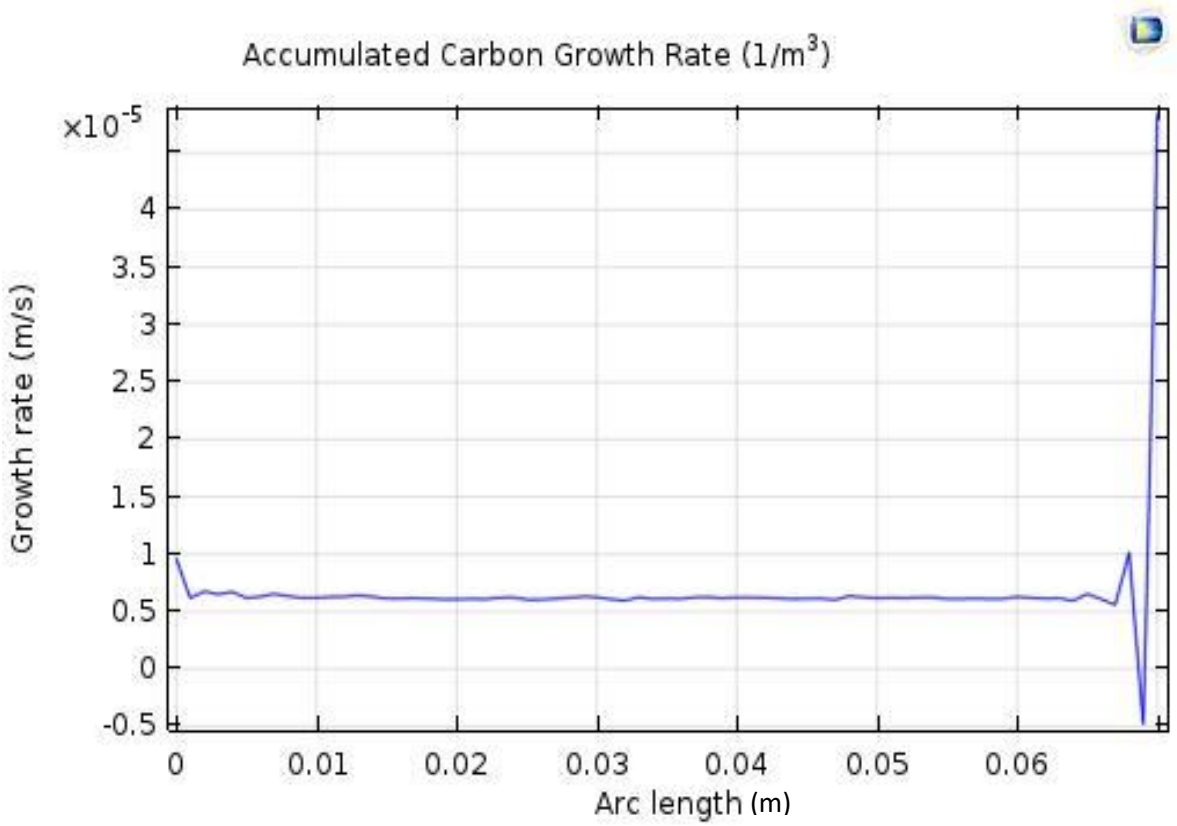

Figure3.7.1 Accumulated carbon growth rate at -50V DC bias at 723K

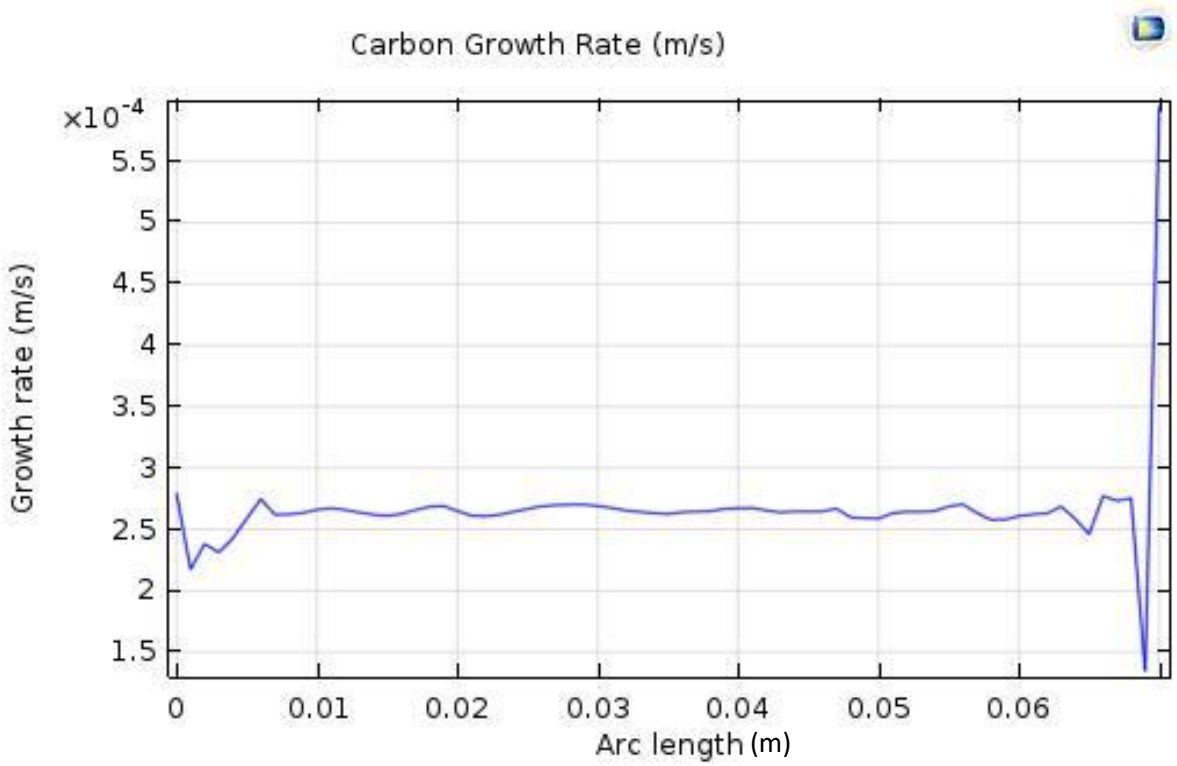

Figure 3.7.2 Accumulated carbon growth rate without bias at 723K

3.2.2) VARYING TEMPERATURE

The simulation for $Ar/C_2H_2/H_2$ gas mixture with nickel as a catalyst is performed at two different temperatures 300K and 723K and a fixed bias of -50V, resulted into formation of irregular two-dimensional nanosheet-like structures on the substrate.

Accumulated Carbon Growth

Typical nanosheets measure 50-60 nm in thickness at 300 K and are seen growing parallel to the substrate surface. It was also observed that the edges of the nanosheet appear to grow vertically up to 220 nm when biasing is applied as shown in Figure 3.9.1 and Figure 3.9.2. The vertical carbon growth along edge resembles vertical graphene-like structure.

At 723 K accumulation and growth of carbon is also observed to be same with a thickness of up to 200 nm parallel to the substrate as shown in Figure

At the edges, vertical growth is observed up to 1 micrometer began due to the tensile stress developed at the boundaries. Due to the combined effect of tensile stress and alignment force exerted by plasma sheath electric field, vertical growth began [34].

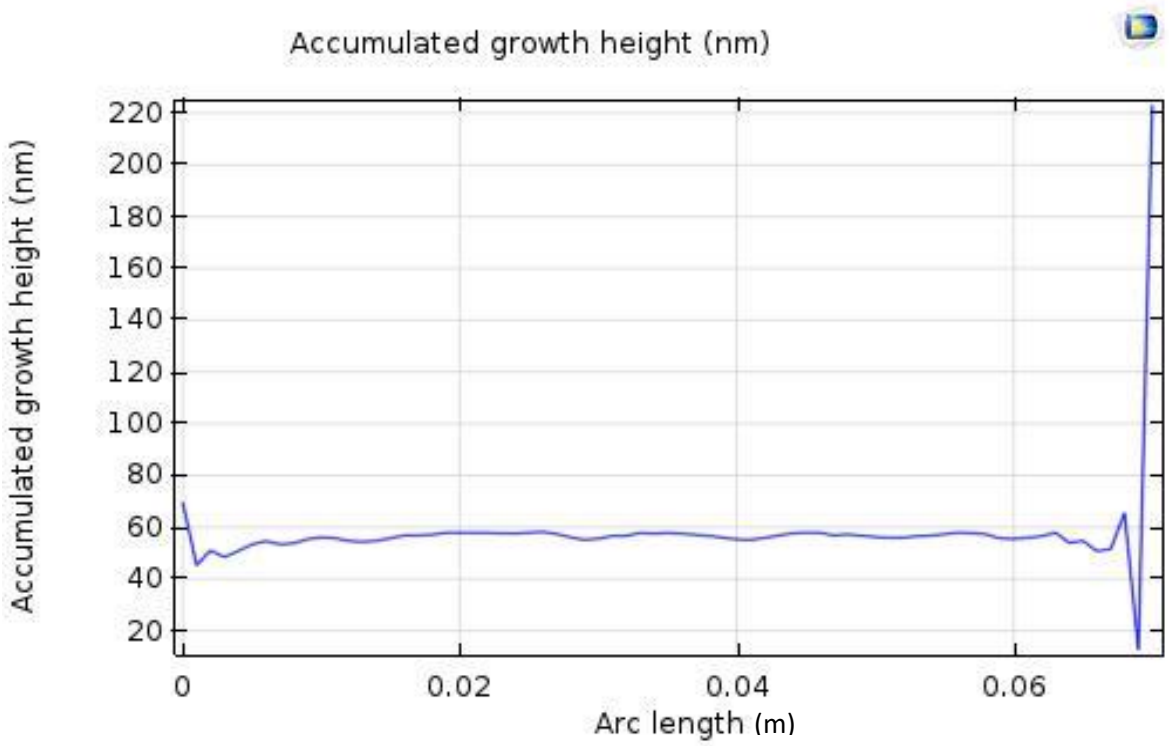

Figure 3.8.1 Accumulated Carbon Growth at 300 K and -50V DC

The thickness of the horizontal graphene sheet increases on increasing temperature because of the effective increase in breaking of constituent gases at the sheet. That leads to more carbon species available for deposition. Also, the thickness of the sheet is non-uniform due to the non-uniform flux of species.

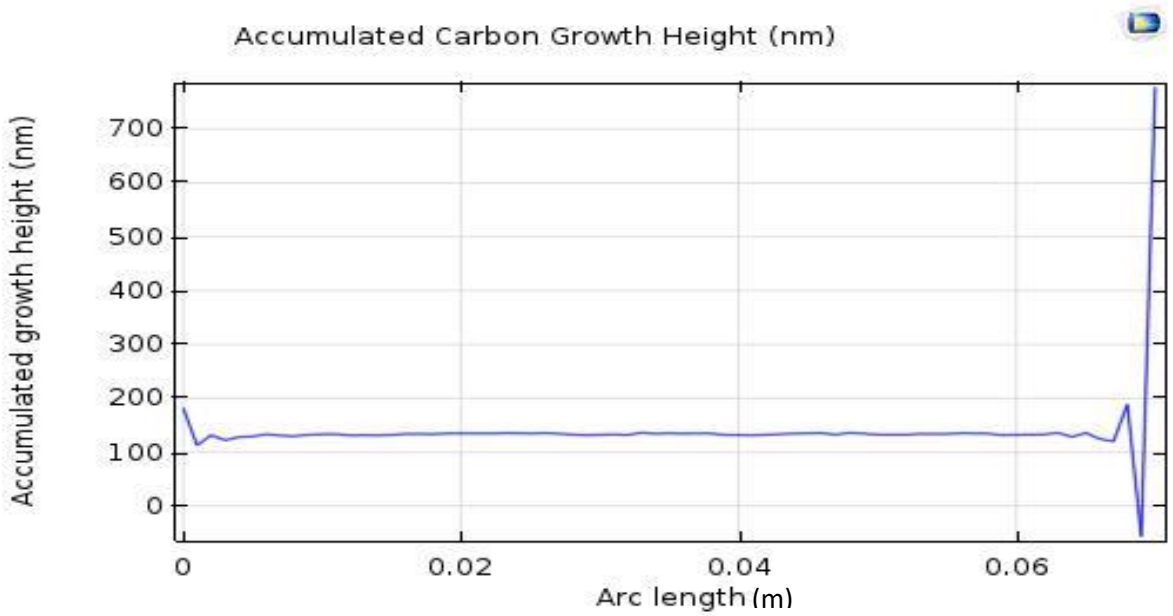

Figure 3.8.2 Accumulated Carbon Growth at 723 K and -50V DC

Accumulated Carbon Growth 3D

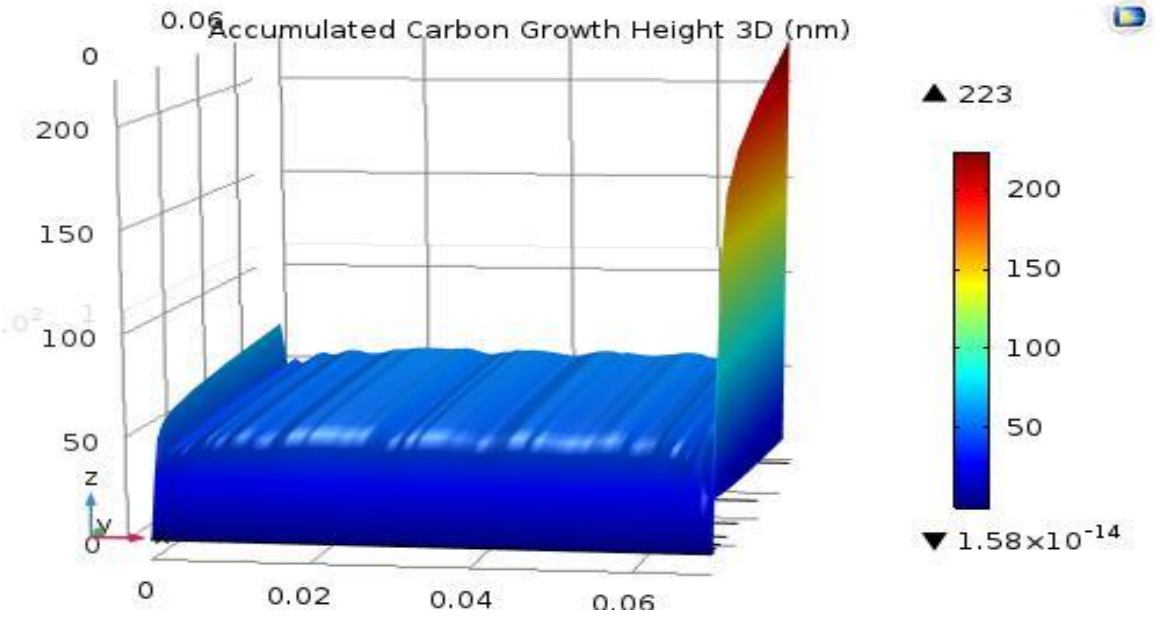

Figure 3.9.1 Accumulated Carbon Growth 3D at 300 K and -50 V DC

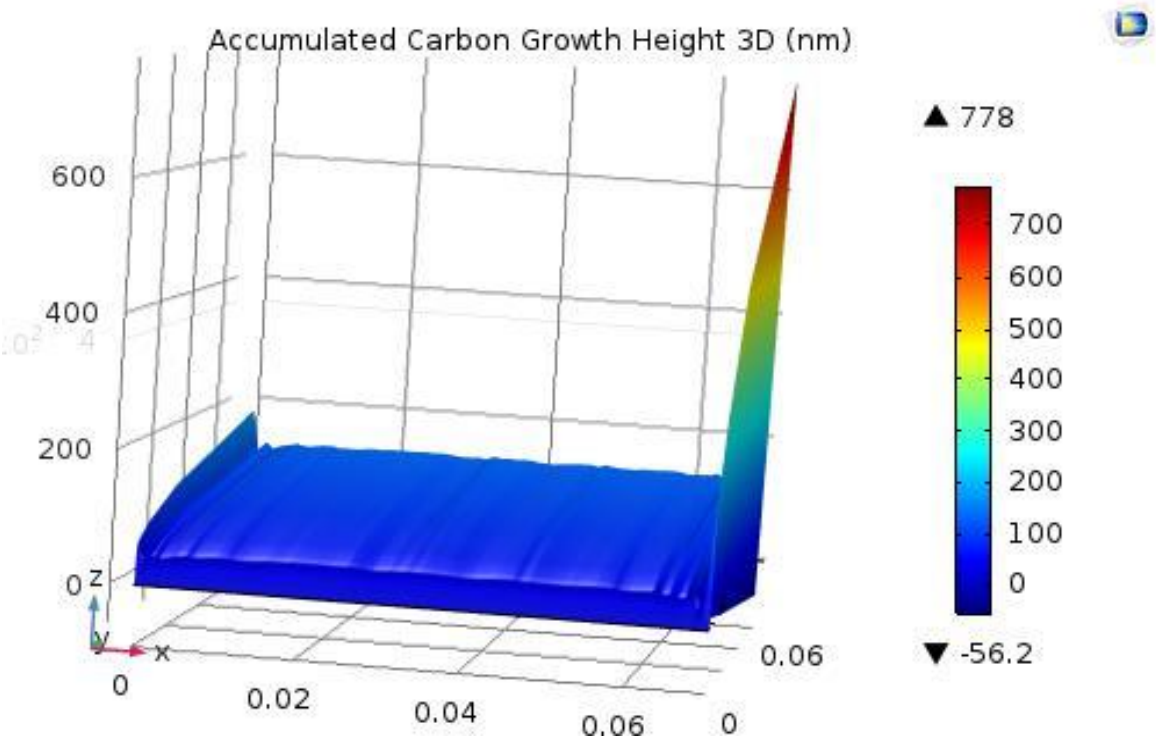

Figure 3.9.2 Accumulated Carbon Growth 3D at 723 K and -50 V DC

Figure 3.10.1 and Figure 3.10.2 shows the 3D accumulated carbon growth on the substrate at 50V(-ve) DC bias and no bias respectively There is a significant 4-fold decrease in carbon growth height on the substrate which makes it suitable for thin film deposition on desired materials.

Accumulated Carbon Growth Rate

The carbon growth rate along the different part of the substrate is not same in both the cases of bias and no bias as shown in Figure 3.11.1 and Figure 3.11.2 respectively. One significance of providing bias is an almost uniform growth rate of carbon along the substrate horizontally except at the edge. But in case of no bias, there is a variable rate of carbon growth along the substrate.

From Figure 3.11.1 and 3.11.2, the growth rate is found to be maximum in case of no bias at around 0.5×10^{-5} m/s to 2.6×10^{-4} m/s along substrate and 6×10^{-5} m/s at the edge and a constant growth rate of 1.5×10^{-6} m/s along substrate and 8×10^{-6} m/s at the edge

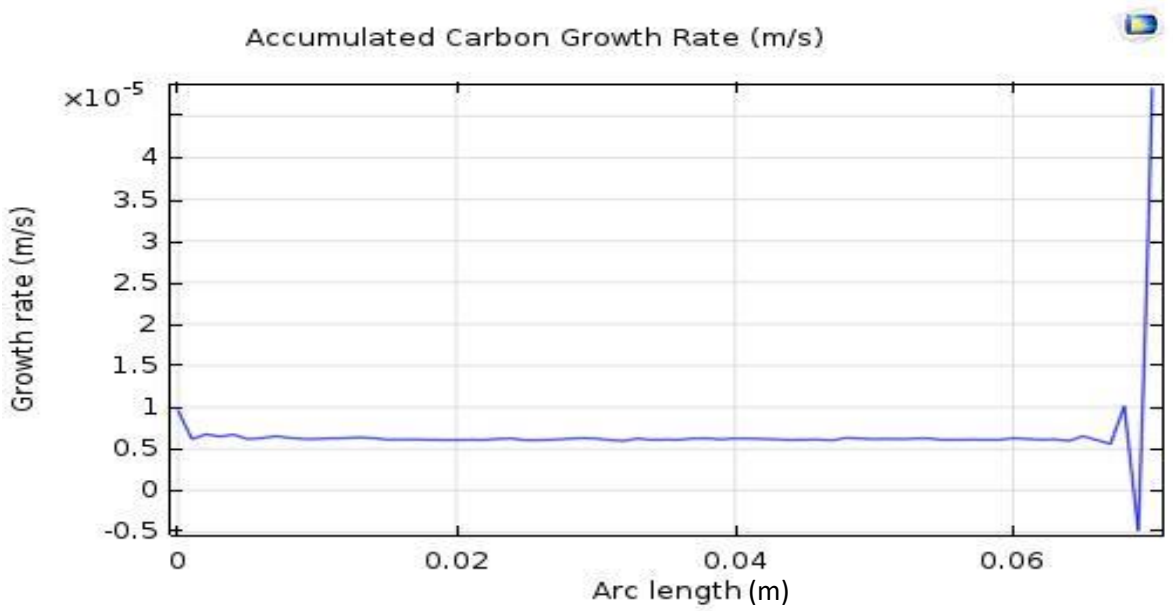

Figure 3.10.1 Accumulated Carbon Growth Rate at 300 K and -50V DC

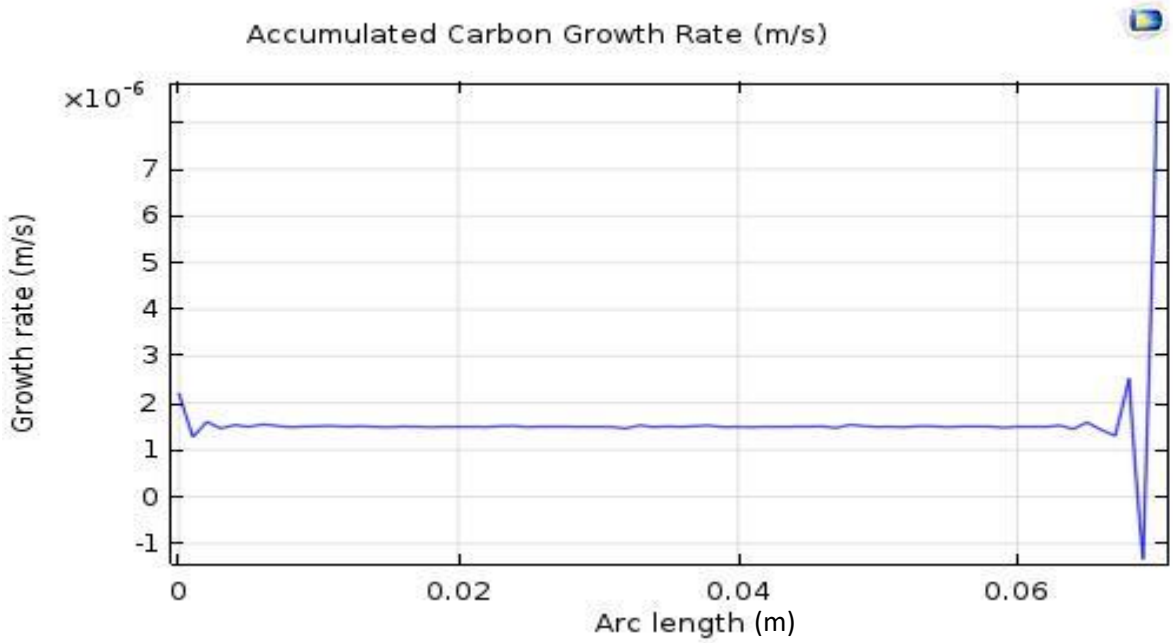

Figure 3.10.2 Accumulated Carbon Growth Rate at 723 K and -50V DC

4

Conclusion

The aim of the project was to simulate the actual experimental conditions of the growth of carbon by PECVD technique using Ar/C2H2/H2 gas mixture and study the parametric effects of various parameters such as biasing and temperature on the growth of graphene,

4.1 Summary

Plasma enhanced CVD techniques is the most suitable synthesis technique for the growth of graphene and thin film deposition compared to other techniques as the temperature attained for the production of plasma is comparatively low as discussed in chapter 1. This advantage plays an important role in the commercial and industrial production of graphene and carbon thin films in semiconductor industries where the fabricating materials cannot withstand high temperature as discussed in chapter 1 and seen from results in chapter 3. The plasma interface of COMSOL simulates the production of plasma of Argon under the effect of applied Radio frequency voltage leading to ionization and chain of electron impact reactions to produce plasma as explained in reaction section and plasma interface section of chapter 2. The heavy species transport section of chapter 2 involves the decomposition of carbon gas Acetylene into various ions and neutrals as shown in reactions Table 4 and species Table 3. The flow of these carbon species towards the substrate is accompanied by either laminar flow or substrate bias as explained in chapter 2.

The planar growth of non-uniform graphene-like structure takes place with an effective thickness ranging from 50-60 nm when the substrate biasing was kept at -50V DC at a temperature of 723K. But there is an 8-fold increase in graphene thickness up to 400nm when no biasing is provided, as can be concluded from the results of chapter 3. At the edges, vertical growth of graphene is observed with a height of 223nm in case of -50V DC bias and 600nm in case of no biasing, as can be observed from the results section of chapter 3.

In chapter 3, the effect of temperature on the growth of graphene is also observed. It can be observed that with an increase in temperature the diffusion of carbon into catalyst nanoparticle increases and ultimately the overall thickness of planar graphene on the substrate and vertical graphene at the edges increases.

4.2 Future outlook

Graphene exhibits astonishing properties for industrial and research purposes having a great potential in electrical and electronic applications such as photovoltaic, electron field emitters, semiconductor devices, sensors, displays, conductors, and energy conversion devices (e.g., fuel cells, harvesters and batteries), energy storage devices such as supercapacitors and storage devices for various fluids

REFERENCES

[1]. W. B. Choi, D. S. Chung, J. H. Kang, H. Y. Kim, Y. W. Jin, I. T. Han, Y. H. Lee, J. E. Jung, N. S. Lee, G. S. Park, and J. M. Kim, Appl. Phys. Lett. (75) 3129 (1999)

[2]. S. J. Tans, A. R. M. Verschueren, and C. Dekker, Nature (London) (49) 331 (1998).

[3]. M. B. Nardelli and J. Bernholc, Phys. Rev. B (60) R16338 (1999).

[4]. L. Nilsson, O. Groening, O. Kuettel, P. Groening, and L. Schlapbach, J. Vac. Sci. Technol. B (20) 326 (2002).

[5]. L. Delzeit, I. McAninch, B. A. Cruden, D. Hash, B. Chen, J. Han, and M. Meyyappan, J. Appl. Phys. (91) 6027 (2002).

[6]. Bin, Y.Z.; Chen, Q.Y.; Nakamura, Y.; Tsuda, K.; Matsuo, M. Preparation, and characterization of carbon films prepared from poly(vinyl alcohol) containing metal oxide and nanofibers with iodine pretreatment. Carbon, (45) 1330–1339, (2007).

[7]. Yang, D.; Xia, L.; Zhao, H.; Hu, X.; Liu, Y.; Li, J.; Wan, X. Preparation and characterization of an ultrathin carbon shell coating a silver core for shell-isolated nanoparticle-enhanced Raman spectroscopy. Chem. Common, (51) (2011)

[8]. Foley, H.C. Carbogenic molecular sieves: Synthesis, properties and applications. Microporous Mater, (4) 407–433, (2005)

[9]. Sheem, K.Y.; Song, E.H.; Lee, Y.H. High-rate charging performance using high-capacity carbon nanofilms coated on alumina nanoparticles for lithium-ion battery anode. Electrochim. Acta, (78) 223–228, (2012).

[10]. Tsang, S.C.; Caps, V.; Paraskevas, I.; Chadwick, D.; Thompsett, D. Magnetically separable, carbon-supported nanocatalysts for the manufacture of fine chemicals. Angew. Chem. Int. Ed. ,(43)5645–5649, (2005).

[11]. S.O. Podgorny, I.P. Demeshko, O.T. Podgornaya, Cadmium telluride nanofilms application in carbon monoxide detection, IEEE (24), 1335-1649 (2007)

[12]. Podgornyi S.O., Podgornaya O.T., Skutin E.D., Demeshko I.P. Lukoyanova O.V, Fedotova K.I., Zinc selenide nanofilms application in carbon monoxide detection, (53) (2016)

[13]. M. Meyyappan, L. Delzeit, A. Cassell, and D. Hash, Plasma Sources Sci. Technol. (12) 205 (2003), and references therein.

[14]. L. Tsakadze, K. Ostrikov, and S. Xu, (in press); Z. Tsakadze, S. Xu, J. Long, and K. Ostrikov, Bull. Am. Phys. Soc. (48) 13 (2003).

[15]. C. Bower, W. Zhu, S. Jin, and O. Zhou, Appl. Phys. Lett. (77) 830 (2000).

[16]. Changgu Lee, Xiaoding Wei1, Jeffrey W. Kysar , James Hone, Measurement of the Elastic Properties and Intrinsic Strength of Monolayer Graphene, Science, 321 (2008).

[17]. Taisuke Ohta, Aaron Bostwick, Thomas Seyller, Karsten Horn, Eli Rotenberg, Controlling the Electronic Structure of Bilayer Graphene, Science, 313 (2006).

[18]. Young-Woo Son, Marvin L. Cohen & Steven G. Louie, Half-metallic graphene Nanoribbons, Nature (444) 347–349 (2006).

[19]. Tsai, S.H., Chiang, F.K., Tsai, T.G., Shieu, F.S., and Shih, H.C. Synthesis and characterization of the aligned hydrogenated amorphous carbon nanotubes by electron cyclotron resonance excitation. Thin Solid Films, 366(1): 11–15. (2000).

[20]. Tomohiro Okumura. Inductively Coupled Plasma Sources and Applications. Physics Research International Volume, (13) 153-159 (2010).

[21]. T. Okumura and I. Nakayama, “New inductively coupled plasma source using a multi-spiral coil," Review of Scientific Instruments, (66)11, 5262–5265, (1995).

[22]. T. G. Beuthe, J. S. Chang, Jpn. J. Appl. Phys., Part 1, (38) 4576, (1991).

[23]. A. Bogaerts, K. de Bleecker, V. Georgieva, I. Kolev, M. Madani, E. Neyts, Plasma Process. Polym, (3) 110 (2010).

[24]. UMIST http://www.udfa.net/

[25]. I. Denysenko, N. A. Azarenkov, J. Phys, D: Appl. Phys., 44(174), 031 (2011).

[26]. I. Denysenko, K. Ostrikov, J. Phys. D Appl. Phys., (42) 015208, (2009).

[27]. Z. Marvi, S. Xu, G. Foroutan, K. Ostrikov, Phys. Plasmas, (22) 013504 (2015)

[28]. I. Denysenko, K. Ostrikov, Appl. Phys. Lett., 90(251), 501(2006).

[29]. H. Mehdipour, K. Ostrikov, A. E. Rider, Nanotechnology, 21(455), 605.

[30]. I. Denysenko, K. Ostrikov, M. Y. Yu, N. A. Azarenkov, J. Appl. Phys. (102) 074308, (2010).

[31]. Richard S. Myers. Collision theory, *J. Chem. Educ* 55(4), 1978,

[32]. M. Gryziński. Theoretical description of collisions in plasma: classical methods. Journal de Physique Colloques, 40 (C7), (1979).

[33]. C. S. Cojocaru, A. Senger, F. L. Normand, J. Nanosci. Nanotech, (23) 213-221 (2006).

[34]. M. Rodriguez, J. Mater. Res., (8) 3233, (1993).

[35]. J. W. G. Wildoer, L. C. Venema, A. G. Rinzler, R. E. Smalley, C. Dekker, Nature, (59) 391 (1998).